



Measurement of the Λ_b cross section and the $\bar{\Lambda}_b$ to Λ_b ratio with $J/\psi\Lambda$ decays in pp collisions at $\sqrt{s} = 7$ TeV

The CMS Collaboration*

Abstract

The Λ_b differential production cross section and the cross-section ratio $\sigma(\bar{\Lambda}_b)/\sigma(\Lambda_b)$ are measured as functions of transverse momentum $p_T^{\Lambda_b}$ and rapidity $|y^{\Lambda_b}|$ in pp collisions at $\sqrt{s} = 7$ TeV using data collected by the CMS experiment at the LHC. The measurements are based on Λ_b decays reconstructed in the exclusive final state $J/\psi\Lambda$, with the subsequent decays $J/\psi \rightarrow \mu^+\mu^-$ and $\Lambda \rightarrow p\pi$, using a data sample corresponding to an integrated luminosity of 1.9 fb^{-1} . The product $\sigma(\Lambda_b) \times \mathcal{B}(\Lambda_b \rightarrow J/\psi\Lambda)$ versus $p_T^{\Lambda_b}$ falls faster than that of b mesons. The measured value of $\sigma(\Lambda_b) \times \mathcal{B}(\Lambda_b \rightarrow J/\psi\Lambda)$ for $p_T^{\Lambda_b} > 10 \text{ GeV}$ and $|y^{\Lambda_b}| < 2.0$ is $1.16 \pm 0.06 \pm 0.12 \text{ nb}$, and the integrated $\sigma(\bar{\Lambda}_b)/\sigma(\Lambda_b)$ ratio is $1.02 \pm 0.07 \pm 0.09$, where the uncertainties are statistical and systematic, respectively.

Submitted to Physics Letters B

*See Appendix A for the list of collaboration members

1 Introduction

Cross sections for b-quark production in high-energy hadronic collisions have been measured at $p\bar{p}$ colliders at center-of-mass energies from 630 GeV [1] to 1.96 TeV [2–4], in fixed-target p-nucleus collisions with beam energies from 800 to 920 GeV [5], and recently in pp collisions at 7 TeV at the Large Hadron Collider (LHC) [6–13]. As the expected cross sections can be calculated in perturbative quantum chromodynamics (QCD), the comparison between data and predictions provides a critical test of next-to-leading-order (NLO) calculations [14, 15].

Considerable progress has been achieved in understanding heavy-quark production at Tevatron energies, largely resolving earlier discrepancies in which theoretical predictions were significantly below observed production rates [15]. However, substantial theoretical uncertainties on production cross sections remain due to the dependence on the renormalization and factorization scales. Measurements of b-hadron production at 7 TeV represent a test of theoretical approaches that aim to describe heavy-flavor production at the new center-of-mass energy [16, 17]. Furthermore, understanding the production rates for b hadrons represents an essential component in accurately estimating heavy-quark backgrounds for various searches, such as $H^0 \rightarrow b\bar{b}$ and supersymmetric or exotic new physics signatures with b quarks.

This Letter presents the first measurement of the production cross section of a b baryon, Λ_b , from fully reconstructed $J/\psi \Lambda$ decays in pp collisions at $\sqrt{s} = 7$ TeV and complements the measurements of B^+ [6], B^0 [7], and B_s^0 [9] production cross sections also performed by the Compact Muon Solenoid (CMS) experiment at the LHC [18]. The comparison of baryon production relative to meson production resulting from the same initial b-quark momentum spectrum allows for tests of differences in the hadronization process. Such differences are particularly interesting in the context of heavy-baryon production in relativistic heavy-ion collisions, where the medium could significantly enhance the production of heavy baryons relative to mesons [19–21]. Furthermore, the pp initial state at the LHC allows tests of baryon transport models, which predict rapidity-dependent antibaryon/baryon asymmetries, in contrast to baryon-antibaryon pair production, which typically results in equal yields [22, 23]. Measurements of the $\bar{\Lambda}_b$ to Λ_b cross-section ratio, $\sigma(\bar{\Lambda}_b)/\sigma(\Lambda_b)$, as functions of $p_T^{\Lambda_b}$ and $|y^{\Lambda_b}|$ allow for the first test of such models with heavy-quark baryons at $\sqrt{s} = 7$ TeV.

Events with Λ_b baryons reconstructed from their decays to the final state $J/\psi \Lambda$, with $J/\psi \rightarrow \mu^+ \mu^-$ and $\Lambda \rightarrow p\pi$, are used to measure the differential cross sections $d\sigma/dp_T^{\Lambda_b} \times \mathcal{B}(\Lambda_b \rightarrow J/\psi \Lambda)$, $d\sigma/dy^{\Lambda_b} \times \mathcal{B}(\Lambda_b \rightarrow J/\psi \Lambda)$, and $\sigma(\bar{\Lambda}_b)/\sigma(\Lambda_b)$ with respect to the transverse momentum $p_T^{\Lambda_b}$ and the rapidity $|y^{\Lambda_b}|$, as well as the integrated cross section times branching fraction for $p_T^{\Lambda_b} > 10$ GeV and $|y^{\Lambda_b}| < 2.0$. The cross section times branching fraction is reported instead of the cross section itself because of the 54% uncertainty on $\mathcal{B}(\Lambda_b \rightarrow J/\psi \Lambda)$ [24]. The cross section times branching fraction measurements are averaged over particle and antiparticle states, while the ratio is computed by distinguishing the two states via decays to p or \bar{p} , respectively.

2 Detector

The data sample used in this analysis was collected by the CMS experiment in 2011 and corresponds to an integrated luminosity of $1.86 \pm 0.04 \text{ fb}^{-1}$ [25]. A detailed description of the detector may be found elsewhere [18]. The main detector components used in this analysis are the silicon tracker and the muon detection systems.

The silicon tracker measures charged particles within the pseudorapidity range $|\eta| < 2.5$, where $\eta = -\ln[\tan(\theta/2)]$ and θ is the polar angle of the track relative to the counterclock-

wise beam direction. It consists of 1440 silicon pixel and 15 148 silicon strip detector modules and is located in the 3.8 T field of the superconducting solenoid. It provides an impact parameter resolution of about $15 \mu\text{m}$ and a p_T resolution of about 1.5% for particles with transverse momenta up to 100 GeV. Muons are measured in the pseudorapidity range $|\eta| < 2.4$, with detection planes made using three technologies: drift tubes, cathode strip chambers, and resistive plate chambers. Events are recorded with a two-level trigger system. The first level is composed of custom hardware processors and uses information from the calorimeters and muon systems to select the most interesting events. The high-level trigger processor farm further decreases the event rate from about 100 kHz to around 350 Hz before data storage.

3 Event selection

Early data taking conditions in 2011 utilized a loose dimuon trigger with the following requirements. Events are selected requiring two oppositely charged muons with dimuon transverse momentum greater than 6.9 GeV. Displaced muon pairs from long-lived b-hadron decays are preferentially selected by further requiring a transverse separation from the mean pp collision position ("beamspot") greater than three times its uncertainty, where the uncertainty incorporates the vertex and beamspot measurements. Also required at the trigger level are a dimuon vertex fit confidence level larger than 0.5% and $\cos \alpha > 0.9$, where α is defined as the angle in the plane transverse to the beams between the dimuon momentum and the vector from the beamspot to the dimuon vertex. The dimuon invariant mass $m_{\mu^+\mu^-}$ is required to satisfy $2.9 < m_{\mu^+\mu^-} < 3.3 \text{ GeV}$. For the later 46% of the dataset, the trigger was tightened by increasing the dimuon vertex fit confidence level threshold to 10% and imposing kinematic requirements of $p_T^\mu > 3.5 \text{ GeV}$ and $|\eta^\mu| < 2.2$ for each of the muons. The remaining 2011 data were recorded with even tighter triggers and are not used in the analysis.

Muon candidates are fully reconstructed by combining information from the silicon tracker [26] and muon detectors, and are required to be within the kinematic acceptance region of $p_T^\mu > 3.5 \text{ GeV}$ and $|\eta^\mu| < 2.2$. Muon candidates are further required to have a track χ^2 per degree of freedom < 1.8 , at least 11 silicon tracker hits, at least two hits in the pixel system, and to be matched to at least one track segment in the muon system. Multiple muon candidates are not allowed to share the same muon track segments [27].

Opposite-sign muon pairs are fit to a common vertex to form J/ψ candidates, which are required to be within 150 MeV of the world-average J/ψ mass [24]. The J/ψ candidates are also required to have p_T greater than 7 GeV, a dimuon vertex fit confidence level larger than 0.5%, $\cos \alpha > 0.95$, and a transverse separation of the vertex from the beamspot greater than three times its uncertainty.

The Λ candidates are formed by fitting oppositely charged tracks to a common vertex. Each track is required to have at least 6 hits in the silicon tracker, a χ^2 per degree of freedom < 5 , and a transverse impact parameter with respect to the beamspot greater than 0.5 times its uncertainty. The proton candidate, identified as the higher-momentum track, is required to have $p_T > 1.0 \text{ GeV}$. Misassignment of the correct proton track is found to be negligible from simulation. The reconstructed Λ decay vertex must have a χ^2 per degree of freedom < 7 and a transverse separation from the beamspot at least five times larger than its uncertainty. The invariant mass $m_{p\pi}$ is required to be within 8 MeV of the world-average Λ mass [24]. Candidates are rejected if $m_{\pi^+\pi^-}$ is within 20 MeV of the world-average K_S^0 mass [24].

The Λ_b candidates are formed by combining a J/ψ candidate with a Λ candidate. A vertex-constrained fit is performed with the two muons and the Λ candidate, with the invariant

masses of the J/ψ and Λ candidates constrained to their world-average values [24]. The Λ_b vertex fit confidence level is required to be greater than 1% and the reconstructed Λ_b mass must satisfy $5.2 < m_{J/\psi\Lambda} < 6.0$ GeV. Multiple Λ_b candidates are found in less than 1% of the events with at least one candidate passing all selection criteria. In those cases, only the candidate with the highest Λ_b vertex fit confidence level is retained. The $m_{J/\psi\Lambda}$ distributions for selected Λ_b and $\bar{\Lambda}_b$ candidates are shown in Fig. 1.

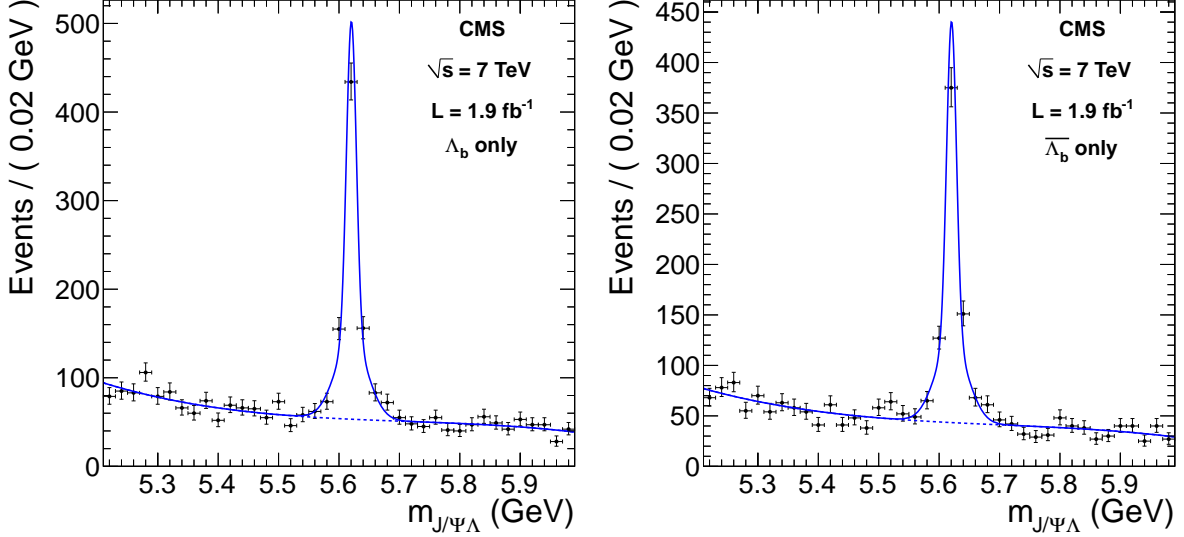


Figure 1: Fit results for the $m_{J/\psi\Lambda}$ distribution for Λ_b (left) and $\bar{\Lambda}_b$ (right) for $p_T^{\Lambda_b} > 10$ GeV and $|y^{\Lambda_b}| < 2.0$, where the dashed line shows the background fit function, the solid line shows the sum of signal and background, and the points indicate the data.

4 Efficiency determination

The efficiency for triggering on and reconstructing Λ_b baryons is computed with a combination of techniques using the data and large samples of fully simulated Monte Carlo (MC) signal events generated with PYTHIA 6.422 [28], decayed by EVTGEN [29], and simulated using GEANT4 [30]. The efficiency is factorized according to

$$\epsilon = \mathcal{A} \cdot \epsilon_{\text{trig}}^{\mu_1} \cdot \epsilon_{\text{trig}}^{\mu_2} \cdot \epsilon_{\text{reco}}^{\mu_1} \cdot \epsilon_{\text{reco}}^{\mu_2} \cdot \epsilon_{\text{trig}}^{\mu\mu} \cdot \epsilon_{\text{sel}}^{\Lambda_b} \quad (1)$$

where each term is described below. The trigger ($\epsilon_{\text{trig}}^{\mu_i}$) and muon-reconstruction efficiencies ($\epsilon_{\text{reco}}^{\mu_i}$) are obtained from a large sample of inclusive $J/\psi \rightarrow \mu^+\mu^-$ decays in data using a “tag-and-probe” technique similar to that described in Ref. [31], where one muon is identified with stringent quality requirements and the second muon is identified using information either exclusively from the tracker (to measure the trigger and offline muon-identification efficiencies) or from the muon system (to measure the trigger and offline tracking efficiencies). While, in principle, the inclusive $J/\psi \rightarrow \mu^+\mu^-$ sample can include signal events, which could bias the measurement, in practice the fraction is negligibly small and provides an unbiased measurement of the muon efficiencies.

For the portion of the trigger efficiency that depends on single-muon requirements ($\epsilon_{\text{trig}}^{\mu_i}$), the efficiency for a given Λ_b event is computed as the product of the two single-muon efficiencies. However, the trigger efficiencies for dimuon events where the muons bend toward each

other are up to 30% lower than for events where the muons bend away from each other for certain portions of the detector. This inefficiency arises when the muon trajectories cross in the muon system, and one of the candidates is rejected because of shared hits. To account for this effect, the trigger efficiencies for muons that bend toward and away from each other are computed separately in data and the appropriate efficiency is applied to each class of signal events. This procedure naturally accounts for the correlations between the two single-muon efficiencies, as confirmed in simulation. The portions of the trigger efficiency that depend on dimuon quantities ($\epsilon_{\text{trig}}^{\mu\mu}$) are measured from an inclusive J/ψ sample collected with triggers where only single-muon requirements are applied.

The probabilities for the muons to lie within the dimuon kinematic acceptance region (\mathcal{A}) and for the Λ_b and $\bar{\Lambda}_b$ candidates to pass the selection requirements ($\epsilon_{\text{sel}}^{\Lambda_b}$) are determined from the simulated events. To minimize the effect of the PYTHIA modeling of the $p_T^{\Lambda_b}$ and $|y^{\Lambda_b}|$ distributions on the acceptance and efficiency calculations, the simulated events are reweighted to match the kinematic distributions observed in the data. The simulated events used for the efficiency calculations have also been reweighted to match the measured distribution of the number of pp interactions per event (pileup). On average, there are six pileup interactions in the data sample used in this analysis. The efficiencies for hadron track reconstruction [32], Λ_b reconstruction [33], and fulfilling the vertex quality requirements are found to be consistent between data and simulation.

The total efficiency of this selection, defined as the fraction of $\Lambda_b \rightarrow J/\psi\Lambda$ with $J/\psi \rightarrow \mu^+\mu^-$ and $\Lambda \rightarrow p\pi$ decays produced with $p_T^{\Lambda_b} > 10$ GeV and $|y^{\Lambda_b}| < 2.0$ that pass all criteria, is 0.73%. The efficiency ranges from 0.3% for $p_T^{\Lambda_b}$ 10–13 GeV to 4.0% for $p_T^{\Lambda_b} > 28$ GeV, with the largest losses due to the Λ reconstruction (10–16% efficiency), the dimuon kinematic acceptance (12–63%), and the displaced dimuon trigger requirements (33–56%). The efficiencies in bins of $p_T^{\Lambda_b}$ and $|y^{\Lambda_b}|$ are shown in Table 1.

To measure the ratio of antiparticle to particle cross sections $\sigma(\bar{\Lambda}_b)/\sigma(\Lambda_b)$, only the ratio of the Λ_b and $\bar{\Lambda}_b$ detection efficiencies is needed. Many of the efficiency contributions cancel in the ratio, including all the J/ψ and μ efficiencies since the particle and antiparticle states are indistinguishable. However, the Λ and $\bar{\Lambda}$ reconstruction efficiencies differ because of different interaction cross sections with the detector material; the \bar{p} are more likely to suffer a nuclear interaction and be lost, resulting in an efficiency that is on average 13% lower for $\bar{\Lambda}_b$ than for Λ_b , as shown in Table 2. The ratio of the Λ_b and $\bar{\Lambda}_b$ selection efficiencies is calculated from simulation as described above for the combined sample, where the simulation modeling of the detector interactions is validated by comparing the number of hits reconstructed on tracks with that observed in data. The uncertainty on the amount of detector material and the appropriateness of simulated interaction cross sections are considered as systematic uncertainties, as described in Section 7.

5 Fitting procedure

The backgrounds are dominated by nonprompt J/ψ production from b hadrons. The dimuon invariant-mass distribution in data confirms that the contamination from events containing a misidentified J/ψ is negligible after all selection criteria have been applied. Background events are distinguished from signal by their reconstructed $m_{J/\psi\Lambda}$ distribution, which is found to be in good agreement between data away from the signal peak and simulated $b \rightarrow J/\psi X$ events. The Λ_b proper decay length distribution in data confirms that the background events arise from long-lived b hadrons, and therefore offers no additional discriminating power between signal

and background. The measured $m_{p\pi}$ distribution shows a purity of 77% genuine Λ events after applying the full selection criteria, while the $m_{\pi^+\pi^-}$ distribution confirms that more than 99.9% of the K_S^0 background is rejected by the kaon mass-window veto.

The Λ_b yields are extracted from unbinned extended maximum-likelihood fits to the $m_{J/\psi\Lambda}$ distribution in bins of $p_T^{\Lambda_b}$ and $|y^{\Lambda_b}|$ defined in Table 1. In each bin, the signal is described by a double-Gaussian function with resolution parameters fixed to values found when fitting simulated signal events and means set to a common value left free in the fit. The background shape is modeled with a third-order polynomial, whose parameters are left free to float independently in each bin. The ratio of antiparticle to particle yields is obtained by simultaneously fitting the Λ_b and $\bar{\Lambda}_b$ mass distributions, with resolution parameters fixed from the fit to the combined Λ_b and $\bar{\Lambda}_b$ simulated sample and common mean allowed to float. The background shapes are fit with separate third-order polynomials, whose parameters are left free in the fit. The signal mass resolution varies as a function of $|y^{\Lambda_b}|$, ranging from a mean of 11 MeV for central Λ_b to 27 MeV for forward Λ_b events.

6 Results

The fitted signal yields in each bin of $p_T^{\Lambda_b}$ and $|y^{\Lambda_b}|$ are summarized in Table 1. Figure 1 shows the fits to the $m_{J/\psi\Lambda}$ distributions for Λ_b and $\bar{\Lambda}_b$ candidates in the inclusive sample with $p_T^{\Lambda_b} > 10$ GeV and $|y^{\Lambda_b}| < 2.0$. The total number of signal events extracted from an inclusive fit is 1252 ± 42 , where the uncertainty is statistical only.

The Λ_b differential cross section times branching fraction is calculated in bins of $p_T^{\Lambda_b}$ as

$$\frac{d\sigma(\text{pp} \rightarrow \Lambda_b X)}{dp_T^{\Lambda_b}} \times \mathcal{B}(\Lambda_b \rightarrow J/\psi\Lambda) = \frac{n_{\text{sig}}}{2 \cdot \epsilon \cdot \mathcal{B} \cdot \mathcal{L} \cdot \Delta p_T^{\Lambda_b}}, \quad (2)$$

and similarly for $|y^{\Lambda_b}|$, where n_{sig} is the fitted number of signal events in the given bin, ϵ is the average efficiency for signal Λ_b and $\bar{\Lambda}_b$ baryons to pass all the selection criteria, \mathcal{L} is the integrated luminosity, $\Delta p_T^{\Lambda_b}$ is the bin size, and \mathcal{B} is the product of branching fractions $\mathcal{B}(J/\psi \rightarrow \mu^+\mu^-) = (5.93 \pm 0.06) \times 10^{-2}$ and $\mathcal{B}(\Lambda \rightarrow p\pi) = 0.639 \pm 0.005$ [24]. The additional factor of two in the denominator accounts for our choice of quoting the cross section for Λ_b production only, while n_{sig} includes both Λ_b and $\bar{\Lambda}_b$. The efficiencies are calculated separately for each bin, always considering only baryons produced with $|y^{\Lambda_b}| < 2.0$ for $p_T^{\Lambda_b}$ bins and $p_T^{\Lambda_b} > 10$ GeV for $|y^{\Lambda_b}|$ bins, and taking into account bin-to-bin migrations (0–2%) because of the finite resolution on the measured $p_T^{\Lambda_b}$ and $|y^{\Lambda_b}|$. Equal production of Λ_b and $\bar{\Lambda}_b$ is assumed for the efficiency, as predicted by PYTHIA and as is consistent with our measurement.

The measured differential cross sections times branching fraction versus $p_T^{\Lambda_b}$ and $|y^{\Lambda_b}|$ are shown in Fig. 2 and Table 1. They are compared to predictions from the NLO MC generator POWHEG 1.0 with the hvq package [34, 35] using a b-quark mass $m_b = 4.75$ GeV, renormalization and factorization scales $\mu = \sqrt{m_b^2 + p_T^2}$, CTEQ6M parton distribution functions [36], and PYTHIA 6.422 [28] for the parton hadronization. The uncertainty on the predicted cross section is calculated by varying the renormalization and factorization scales by factors of two and, independently, m_b by ± 0.25 GeV. The largest variation in each direction is taken as the uncertainty. The data are also compared to the PYTHIA 6.422 prediction, using a b-quark mass of 4.80 GeV, CTEQ6L1 parton distribution functions, and the Z2 tune [37] to simulate the underlying event. No attempt has been made to quantify the uncertainty on the PYTHIA predictions.

Table 1: $\Lambda_b + \bar{\Lambda}_b$ signal yield n_{sig} , efficiency ϵ , and measured differential cross sections times branching fraction $d\sigma/dp_T^{\Lambda_b} \times \mathcal{B}(\Lambda_b \rightarrow J/\psi\Lambda)$ and $d\sigma/dy^{\Lambda_b} \times \mathcal{B}(\Lambda_b \rightarrow J/\psi\Lambda)$, compared to the POWHEG [34, 35] and PYTHIA [28] predictions. The uncertainties on the signal yields are statistical only, while those on the efficiencies are systematic. The uncertainties in the measured cross sections are statistical and systematic, respectively, excluding the common luminosity (2.2%) and branching fraction (1.3%) uncertainties. The POWHEG and PYTHIA predictions also have uncertainties of 54% due to $\mathcal{B}(\Lambda_b \rightarrow J/\psi\Lambda)$, which are not shown.

| $p_T^{\Lambda_b}$ (GeV) | n_{sig} events | ϵ (%) | $d\sigma/dp_T^{\Lambda_b} \times \mathcal{B}(\Lambda_b \rightarrow J/\psi\Lambda)$ (pb/GeV) | POWHEG (pb/GeV) | PYTHIA (pb/GeV) |
|----------------------------|----------------------------|-------------------|--|------------------------|--------------------|
| 10 – 13 | 293 ± 22 | 0.29 ± 0.03 | $240 \pm 20 \pm 30$ | 110^{+40}_{-30} | 210 |
| 13 – 15 | 240 ± 18 | 0.79 ± 0.08 | $108 \pm 8 \pm 12$ | 54^{+21}_{-12} | 102 |
| 15 – 18 | 265 ± 19 | 1.54 ± 0.16 | $41 \pm 3 \pm 4$ | 29^{+10}_{-6} | 55 |
| 18 – 22 | 207 ± 16 | 2.34 ± 0.23 | $15.6 \pm 1.2 \pm 1.6$ | $13.4^{+4.5}_{-2.7}$ | 24.0 |
| 22 – 28 | 145 ± 14 | 3.21 ± 0.34 | $5.3 \pm 0.5 \pm 0.6$ | $5.3^{+1.6}_{-1.1}$ | 9.3 |
| 28 – 50 | 87 ± 11 | 3.96 ± 0.50 | $0.70 \pm 0.09 \pm 0.09$ | $0.89^{+0.32}_{-0.15}$ | 1.42 |
| $ y^{\Lambda_b} $ | n_{sig} events | ϵ (%) | $d\sigma/dy^{\Lambda_b} \times \mathcal{B}(\Lambda_b \rightarrow J/\psi\Lambda)$ (pb) | POWHEG (pb) | PYTHIA (pb) |
| 0.0 – 0.3 | 233 ± 17 | 0.74 ± 0.09 | $370 \pm 30 \pm 50$ | 180^{+70}_{-40} | 330 |
| 0.3 – 0.6 | 256 ± 18 | 0.77 ± 0.09 | $390 \pm 30 \pm 50$ | 170^{+60}_{-40} | 330 |
| 0.6 – 0.9 | 206 ± 16 | 0.81 ± 0.09 | $300 \pm 20 \pm 30$ | 170^{+60}_{-40} | 320 |
| 0.9 – 1.2 | 196 ± 17 | 0.70 ± 0.08 | $330 \pm 30 \pm 40$ | 160^{+60}_{-40} | 300 |
| 1.2 – 1.5 | 189 ± 17 | 0.67 ± 0.09 | $330 \pm 30 \pm 50$ | 150^{+50}_{-40} | 280 |
| 1.5 – 2.0 | 162 ± 18 | 0.65 ± 0.09 | $180 \pm 20 \pm 30$ | 130^{+50}_{-30} | 250 |

The measured p_T spectrum falls faster than predicted by POWHEG and PYTHIA, while the $|y|$ spectrum shape is in agreement with the predictions within uncertainties, as illustrated in the data-to-POWHEG ratio plots shown in the lower panels of Fig. 2. The integrated cross section $\sigma(\text{pp} \rightarrow \Lambda_b X) \times \mathcal{B}(\Lambda_b \rightarrow J/\psi\Lambda)$ for $p_T^{\Lambda_b} > 10 \text{ GeV}$ and $|y^{\Lambda_b}| < 2.0$, calculated as the sum over all p_T bins, is $1.16 \pm 0.06 \pm 0.12 \text{ nb}$, where the first uncertainty is statistical, and the second is systematic. For the total cross section result, the highest $p_T^{\Lambda_b}$ bin is fit without an upper bound and has a yield of 97.0 ± 13.2 events. The total cross section measurement is in good agreement with the prediction from PYTHIA of $1.19 \pm 0.64 \text{ nb}$ and higher than the prediction from POWHEG of $0.63^{+0.41}_{-0.37} \text{ nb}$, where the uncertainties are dominated by the 54% uncertainty on $\mathcal{B}(\Lambda_b \rightarrow J/\psi\Lambda)$ [24].

This result can be compared to previous CMS measurements of B^+ [6], B^0 [7], and B_s^0 [9] production at $\sqrt{s} = 7 \text{ TeV}$. To facilitate the comparison, the B^+ and B^0 results are taken for the range $p_T^B > 10 \text{ GeV}$. Simulated events are generated with MC@NLO [38] with $m_b = 4.75 \text{ GeV}$ and CTEQ6M parton distribution functions to determine the fraction of B^+ , B^0 , and B_s^0 events within the p_T^B and $|y^B|$ ranges used for their respective measurements with the $p_T > 10 \text{ GeV}$ and $|y| < 2.0$ requirements used in this analysis. Scaling by the appropriate ratio and using the world-average values of $\mathcal{B}(\Lambda_b \rightarrow J/\psi\Lambda) = (5.7 \pm 3.1) \times 10^{-4}$ and $\mathcal{B}(B_s^0 \rightarrow J/\psi\phi) = (1.4 \pm 0.5) \times 10^{-3}$ [24], we determine the following cross sections for $p_T^B > 10 \text{ GeV}$ and $|y^B| < 2.0$: $\sigma(\text{pp} \rightarrow B^+ X) = 6.7 \pm 1.0 \mu\text{b}$; $\sigma(\text{pp} \rightarrow B^0 X) = 6.7 \pm 0.8 \mu\text{b}$; $\sigma(\text{pp} \rightarrow B_s^0 X) = 2.5 \pm 1.0 \mu\text{b}$ and $\sigma(\text{pp} \rightarrow \Lambda_b X) = 2.1 \pm 1.1 \mu\text{b}$, where the uncertainties are the quadrature sum of the

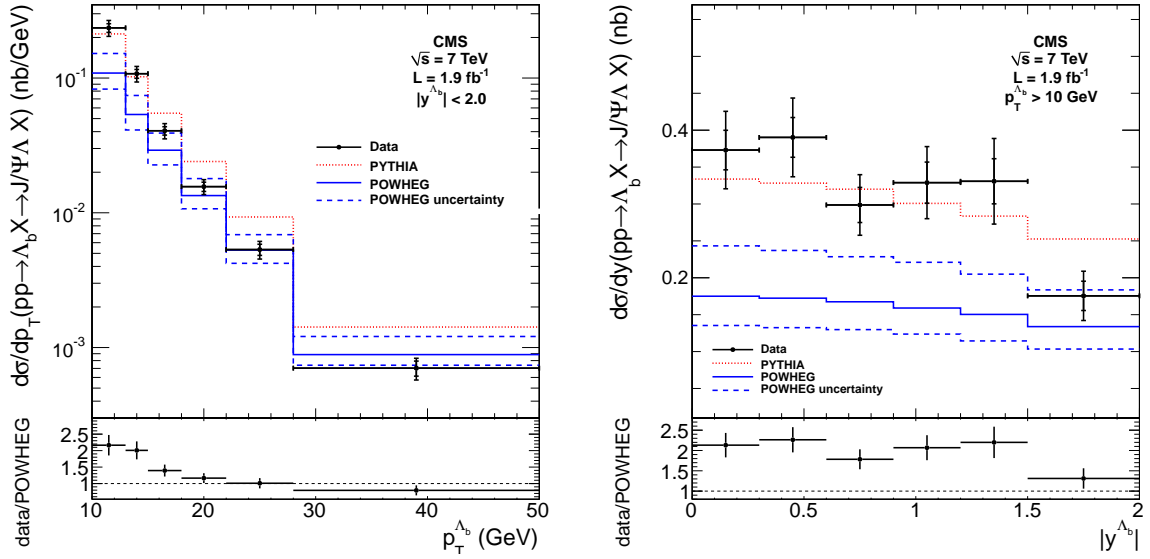


Figure 2: Upper: Measured differential cross sections times branching fraction $d\sigma/dp_T^{\Lambda_b} \times \mathcal{B}(\Lambda_b \rightarrow J/\psi\Lambda)$ (left) and $d\sigma/dy^{\Lambda_b} \times \mathcal{B}(\Lambda_b \rightarrow J/\psi\Lambda)$ (right) compared to the theoretical predictions from PYTHIA and POWHEG. The inner error bars correspond to the statistical uncertainties and the outer ones represent the uncorrelated systematic uncertainties added in quadrature to the statistical uncertainties. The dashed lines show the uncertainties on the POWHEG predictions. Overall uncertainties of 2.2% for the luminosity and 1.3% for the $J/\psi \rightarrow \mu^+\mu^-$ and $\Lambda \rightarrow p\pi$ branching fractions for the data are not shown, nor is the 54% uncertainty due to $\mathcal{B}(\Lambda_b \rightarrow J/\psi\Lambda)$ for the PYTHIA and POWHEG predictions. Lower: The ratio of the measured values to the POWHEG predictions. The error bars include the statistical and uncorrelated systematic uncertainties on the data and the shape-only uncertainties on the POWHEG predictions.

statistical and systematic components. No uncertainty has been included for the phase-space extrapolation based on MC@NLO [38]. The large systematic uncertainties for $\sigma(pp \rightarrow B_s^0 X)$ and $\sigma(pp \rightarrow \Lambda_b X)$ are dominated by the poorly known branching fractions $\mathcal{B}(\Lambda_b \rightarrow J/\psi\Lambda)$ and $\mathcal{B}(B_s^0 \rightarrow J/\psi\phi)$, respectively. The ratios among the four results are in good agreement with the world-average b-quark fragmentation results [24].

The world-average b-quark fragmentation results assume that the fractions are the same for b jets originating from Z decays at LEP and directly from $p\bar{p}$ collisions at the Tevatron. However, measurements of f_{Λ_b} performed at LEP [39, 40] and at the Tevatron [41] show discrepancies. A recent result [42] from the LHCb Collaboration measures a strong p_T dependence of the ratio of Λ_b production to B-meson production, $f_{\Lambda_b}/(f_u + f_d)$, with $f_{\Lambda_b} \equiv \mathcal{B}(b \rightarrow \Lambda_b)$ and $f_q \equiv \mathcal{B}(b \rightarrow B_q)$. Larger f_{Λ_b} values are observed at lower p_T , which suggests that the discrepancy observed between the LEP and Tevatron data may be due to the lower p_T of the Λ_b baryons produced at the Tevatron.

A comparison of this and previous CMS results for b-hadron production versus p_T is shown in the left plot of Fig. 3, where the data are fit to the Tsallis function [43],

$$\frac{1}{N} \frac{dN}{dp_T} = C p_T \left[1 + \frac{\sqrt{p_T^2 + m^2} - m}{nT} \right]^{-n}. \quad (3)$$

Here C is a normalization parameter, T and n are shape parameters, m is the mass of the b hadron and N is the b-hadron yield. The statistical and bin-to-bin systematic uncertainties are

used in the fits. The T parameter represents the inverse slope parameter of an exponential, which dominates at low p_T . Since our data do not constrain that region well, T is fixed to the mean value found from fitting the B^+ and B^0 distributions, where the p_T threshold is lowest. The result of $T = 1.10$ GeV is used to obtain the following values of the n parameter, which controls the power-law behavior at high p_T : $n(B^+) = 5.5 \pm 0.3$, $n(B^0) = 5.8 \pm 0.3$, $n(B_s^0) = 6.6 \pm 0.4$, and $n(\Lambda_b) = 7.6 \pm 0.4$. The larger n value for Λ_b indicates a more steeply falling p_T distribution than observed for the mesons, also suggesting that the production of Λ_b baryons, relative to B mesons, varies as a function of p_T , with a larger Λ_b/B ratio at lower transverse momentum. The right plot of Fig. 3 shows the $p_T^{\Lambda_b}$ spectrum shape compared to B^+ and B^0 , where the distributions are normalized to the common bin with $p_T = 10\text{--}13$ GeV.

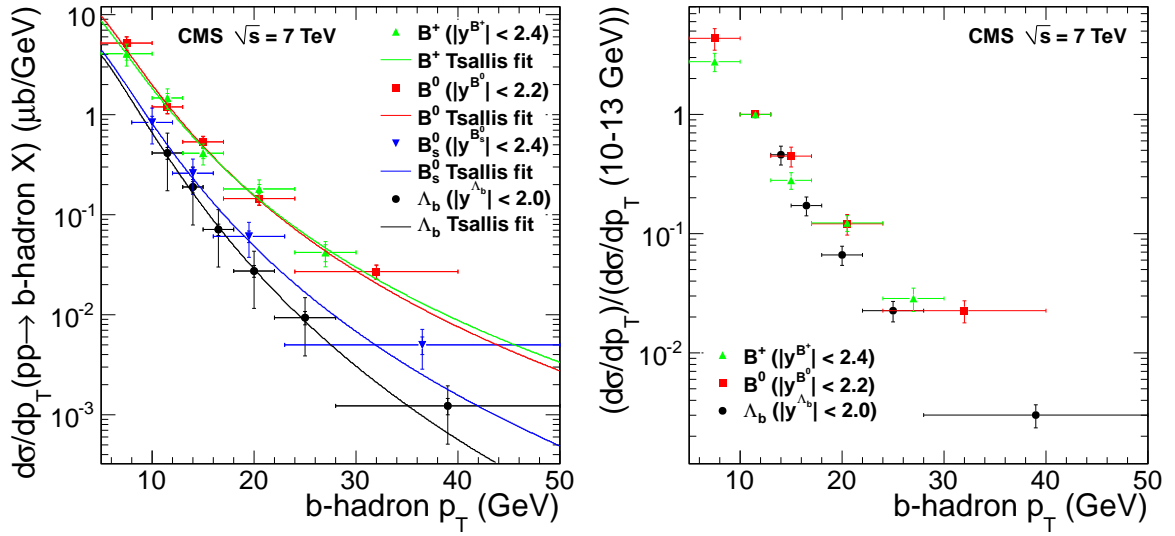


Figure 3: Comparison of production rates for B^+ [6], B^0 [7], B_s^0 [9], and Λ_b versus p_T . The left plot shows the absolute comparison, where the inner error bars correspond to the total bin-to-bin uncertainties, while the outer error bars represent the total bin-to-bin and normalization uncertainties added in quadrature. Fits to the Tsallis function [43] for each distribution are also shown. The overall uncertainties for B_s^0 and Λ_b are dominated by large uncertainties on $\mathcal{B}(B_s^0 \rightarrow J/\psi\phi)$ and $\mathcal{B}(\Lambda_b \rightarrow J/\psi\Lambda)$, respectively. The right plot shows a shape-only comparison where the data are normalized to the 10–13 GeV bin in p_T and the error bars show the bin-to-bin uncertainties only. B_s^0 is omitted because the 10–13 GeV bin is not available for the common normalization.

The ratio $\sigma(\bar{\Lambda}_b)/\sigma(\Lambda_b)$ is calculated in bins of $p_T^{\Lambda_b}$ or $|y^{\Lambda_b}|$ as

$$\sigma(\bar{\Lambda}_b)/\sigma(\Lambda_b) = \frac{n_{\text{sig}}^{\bar{\Lambda}_b}}{n_{\text{sig}}^{\Lambda_b}} \times \frac{\epsilon(\Lambda_b)}{\epsilon(\bar{\Lambda}_b)}, \quad (4)$$

where $n_{\text{sig}}^{\bar{\Lambda}_b}$ and $n_{\text{sig}}^{\Lambda_b}$ are the antiparticle and particle yields in a given bin, and $\epsilon(\Lambda_b)$ and $\epsilon(\bar{\Lambda}_b)$ are the particle and antiparticle efficiencies for a given bin, always considering only baryons produced with $|y^{\Lambda_b}| < 2.0$ for $p_T^{\Lambda_b}$ bins and $p_T^{\Lambda_b} > 10$ GeV for $|y^{\Lambda_b}|$ bins. The results versus $p_T^{\Lambda_b}$ and $|y^{\Lambda_b}|$ are shown in Fig. 4 and Table 2. The ratio $\sigma(\bar{\Lambda}_b)/\sigma(\Lambda_b)$ is found to be consistent with unity and constant as a function of both $p_T^{\Lambda_b}$ and $|y^{\Lambda_b}|$, within the uncertainties, as predicted by POWHEG and PYTHIA. Therefore, no evidence of increased baryon production at forward

pseudorapidities is observed within the available statistical precision for the kinematic regime investigated. The integrated $\sigma(\bar{\Lambda}_b)/\sigma(\Lambda_b)$ for $p_T^{\Lambda_b} > 10$ GeV and $|y^{\Lambda_b}| < 2.0$ is $1.02 \pm 0.07 \pm 0.09$, where the first uncertainty is statistical and the second is systematic.

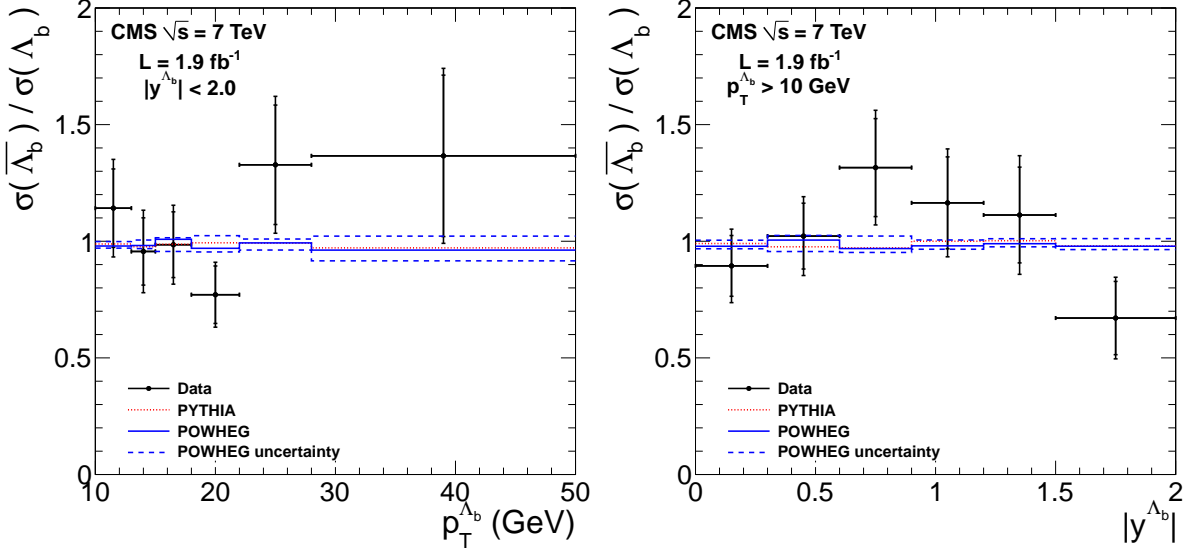


Figure 4: Measured $\sigma(\bar{\Lambda}_b)/\sigma(\Lambda_b)$ (points) versus $p_T^{\Lambda_b}$ (left) and $|y^{\Lambda_b}|$ (right), compared to the theoretical predictions from PYTHIA (red dashed line) and POWHEG (blue solid line). The inner error bars correspond to the statistical uncertainties, and the outer error bars represent the uncorrelated systematic uncertainties added in quadrature to the statistical uncertainties. The dashed blue lines show the uncertainties of the POWHEG predictions.

7 Systematic uncertainties

The cross section is affected by systematic uncertainties on the signal yields and efficiencies that are uncorrelated bin-to-bin and can affect the shapes of the distributions, and by the uncertainties on branching fractions and integrated luminosity, which are common to all bins and only affect the overall normalization. The uncertainties on the signal yields arise from the following sources:

- Signal shape uncertainty (1–6%): evaluated from the variations when floating the means of the two Gaussians (set to a common value) in data or by using a single Gaussian shape.
- Background shape uncertainty (1–2%): evaluated from the variation when using a second-order polynomial, exponential, or third-order polynomial fit in the restricted range 5.4–6.0 GeV.
- Final-state radiation (0–1%): evaluated by removing it from the simulation and taking half of the difference in the results.

The uncertainties on the efficiencies arise from the following sources:

- Pion/proton/ Λ reconstruction efficiency uncertainty (8%): evaluated by varying the simulated detector material [44], alignment, and beamspot position, and by varying the reconstruction cuts, by using different event simulations, and comparing the measured Λ lifetime [33], which is sensitive to the efficiency correction, to the world-

Table 2: Uncorrected signal yield ratio $n_{\text{sig}}^{\bar{\Lambda}_b}/n_{\text{sig}}^{\Lambda_b}$, efficiency ratio $\epsilon(\bar{\Lambda}_b)/\epsilon(\Lambda_b)$, and efficiency-corrected ratio $\sigma(\bar{\Lambda}_b)/\sigma(\Lambda_b)$, compared to the POWHEG [34, 35] and PYTHIA [28] predictions for the corrected ratio. The uncertainties in the corrected ratio are statistical and systematic, respectively. The uncertainties on the uncorrected yield ratio are statistical only and on the efficiency ratio are systematic only.

| $p_T^{\Lambda_b}$ (GeV) | Uncorrected | | Data | POWHEG | PYTHIA |
|-------------------------|---|---|---|---|---|
| | $n_{\text{sig}}^{\bar{\Lambda}_b}/n_{\text{sig}}^{\Lambda_b}$ | $\epsilon(\bar{\Lambda}_b)/\epsilon(\Lambda_b)$ | $\sigma(\bar{\Lambda}_b)/\sigma(\Lambda_b)$ | $\sigma(\bar{\Lambda}_b)/\sigma(\Lambda_b)$ | $\sigma(\bar{\Lambda}_b)/\sigma(\Lambda_b)$ |
| 10–13 | 0.96 ± 0.14 | 0.84 ± 0.09 | $1.14 \pm 0.17 \pm 0.12$ | $0.98^{+0.02}_{-0.01}$ | 0.99 |
| 13–15 | 0.76 ± 0.11 | 0.79 ± 0.09 | $0.96 \pm 0.14 \pm 0.10$ | $0.98^{+0.02}_{-0.01}$ | 0.98 |
| 15–18 | 0.89 ± 0.13 | 0.90 ± 0.09 | $0.98 \pm 0.14 \pm 0.09$ | $1.01^{+0.01}_{-0.05}$ | 0.99 |
| 18–22 | 0.73 ± 0.12 | 0.95 ± 0.08 | $0.77 \pm 0.12 \pm 0.07$ | $0.97^{+0.05}_{-0.02}$ | 0.99 |
| 22–28 | 1.26 ± 0.24 | 0.94 ± 0.10 | $1.33 \pm 0.26 \pm 0.14$ | $0.99^{+0.02}_{-0.03}$ | 0.99 |
| 28–50 | 0.99 ± 0.25 | 0.72 ± 0.08 | $1.37 \pm 0.35 \pm 0.14$ | $0.96^{+0.06}_{-0.04}$ | 0.97 |
| $ y^{\Lambda_b} $ | Uncorrected | | Data | POWHEG | PYTHIA |
| | $n_{\text{sig}}^{\bar{\Lambda}_b}/n_{\text{sig}}^{\Lambda_b}$ | $\epsilon(\bar{\Lambda}_b)/\epsilon(\Lambda_b)$ | $\sigma(\bar{\Lambda}_b)/\sigma(\Lambda_b)$ | $\sigma(\bar{\Lambda}_b)/\sigma(\Lambda_b)$ | $\sigma(\bar{\Lambda}_b)/\sigma(\Lambda_b)$ |
| 0.0–0.3 | 0.71 ± 0.10 | 0.79 ± 0.08 | $0.89 \pm 0.13 \pm 0.09$ | $0.98^{+0.02}_{-0.01}$ | 0.99 |
| 0.3–0.6 | 0.92 ± 0.13 | 0.90 ± 0.08 | $1.02 \pm 0.14 \pm 0.09$ | $1.01^{+0.01}_{-0.05}$ | 0.98 |
| 0.6–0.9 | 1.16 ± 0.18 | 0.88 ± 0.09 | $1.32 \pm 0.21 \pm 0.13$ | $0.97^{+0.05}_{-0.02}$ | 0.97 |
| 0.9–1.2 | 0.99 ± 0.17 | 0.85 ± 0.09 | $1.16 \pm 0.20 \pm 0.12$ | $0.98^{+0.03}_{-0.02}$ | 1.00 |
| 1.2–1.5 | 0.92 ± 0.17 | 0.82 ± 0.11 | $1.11 \pm 0.20 \pm 0.15$ | $0.99^{+0.02}_{-0.01}$ | 1.00 |
| 1.5–2.0 | 0.66 ± 0.16 | 0.99 ± 0.11 | $0.67 \pm 0.16 \pm 0.08$ | $0.98^{+0.03}_{-0.02}$ | 0.98 |

average value [24].

- Tag-and-probe statistical uncertainties (4–6%): evaluated by propagating statistical uncertainties from the data-driven determination of the single-muon efficiencies.
- Tag-and-probe systematic uncertainties (1–7%): evaluated as the difference between the true efficiency in simulation and the efficiency calculated with the tag-and-probe procedure applied to simulated events.
- Statistical precision of the simulated event samples (3–4%): calculated for the dimuon acceptance and reconstruction efficiencies.
- Simulation modeling of the Λ_b kinematic distributions (0–5%): evaluated as half of the difference due to the kinematic reweighting.
- GEANT4 \bar{p} cross section (1–4%): evaluated by considering an alternative cross section model in GEANT4 (CHIPS) [30] for \bar{p} cross sections for interacting with material in the detector [45] and taking the difference in the efficiency as a systematic uncertainty.
- Unknown Λ_b polarization (1–4%): evaluated by generating samples of events with the Λ_b spin fully aligned or anti-aligned with the normal to the plane defined by the Λ_b momentum and the pp beam direction in the laboratory frame and taking the average difference in the efficiency when compared to the nominal analysis, which is performed with unpolarized simulated events.
- Pileup (0–4%): evaluated by varying the number of pileup interactions in simulated events by the uncertainty of the measured pileup interaction distribution.
- Muon kinematics (0–2%): evaluated as the difference in the simulated efficiency when reweighting the muon p_T to match the distribution measured with muons from the inclusive J/ψ sample used in the tag-and-probe measurements.
- Effect of events migrating between p_T and y bins due to resolution (0–1%): evaluated as half of the correction deduced from simulated events.

The bin-to-bin systematic uncertainty is computed as the sum in quadrature of the individual uncertainties and is summarized in Table 1. In addition, there are normalization uncertainties of 2.2% from the luminosity measurement [25] and of 1.3% from the $J/\psi \rightarrow \mu^+\mu^-$ and $\Lambda \rightarrow p\pi$ branching fractions [24]. For the total cross section result computed from the sum of p_T bins, only the signal and background shapes, and the tag-and-probe and simulation statistical uncertainties are treated as uncorrelated. As bin-to-bin correlations cannot be ruled out for the remaining sources of systematic uncertainty, the contribution in each p_T bin is added linearly to compute the sum to ensure that the uncertainty is not underestimated.

Many of these systematic effects cancel in the $\sigma(\bar{\Lambda}_b)/\sigma(\Lambda_b)$ ratio measurement. The remaining uncertainties are from the signal shape (2–8%), background shape (1–3%), GEANT4 \bar{p} cross section (1–7%), variation of detector material (5%), and statistical precision of the simulated samples (6–8%), which are evaluated as described above. The total systematic uncertainty is computed as the quadrature sum of the individual uncertainties and is summarized in Table 2.

8 Conclusions

In summary, the first measurements of the differential cross sections times branching fraction $d\sigma/dp_T^{\Lambda_b} \times \mathcal{B}(\Lambda_b \rightarrow J/\psi\Lambda)$ and $d\sigma/dy^{\Lambda_b} \times \mathcal{B}(\Lambda_b \rightarrow J/\psi\Lambda)$ for Λ_b baryons produced in pp collisions at $\sqrt{s} = 7$ TeV have been presented. The measurements are given for $p_T^{\Lambda_b} > 10$ GeV and

$|y^{\Lambda_b}| < 2.0$. The $p_T^{\Lambda_b}$ distribution falls faster than both the measured p_T spectra from b mesons and the predicted spectra from the NLO MC POWHEG and the leading-order MC PYTHIA. The total cross section and rapidity distribution are consistent with both predictions within large uncertainties. The measured $\sigma(\overline{\Lambda}_b)/\sigma(\Lambda_b)$ ratio is consistent with unity and constant as a function of both $p_T^{\Lambda_b}$ and $|y^{\Lambda_b}|$.

Acknowledgments

We congratulate our colleagues in the CERN accelerator departments for the excellent performance of the LHC machine. We thank the technical and administrative staff at CERN and other CMS institutes, and acknowledge support from: FMSR (Austria); FNRS and FWO (Belgium); CNPq, CAPES, FAPERJ, and FAPESP (Brazil); MES (Bulgaria); CERN; CAS, MoST, and NSFC (China); COLCIENCIAS (Colombia); MSES (Croatia); RPF (Cyprus); MoER, SF0690030s09 and ERDF (Estonia); Academy of Finland, MEC, and HIP (Finland); CEA and CNRS/IN2P3 (France); BMBF, DFG, and HGF (Germany); GSRT (Greece); OTKA and NKTH (Hungary); DAE and DST (India); IPM (Iran); SFI (Ireland); INFN (Italy); NRF and WCU (Korea); LAS (Lithuania); CINVESTAV, CONACYT, SEP, and UASLP-FAI (Mexico); MSI (New Zealand); PAEC (Pakistan); MSHE and NSC (Poland); FCT (Portugal); JINR (Armenia, Belarus, Georgia, Ukraine, Uzbekistan); MON, RosAtom, RAS and RFBR (Russia); MSTD (Serbia); MICINN and CPAN (Spain); Swiss Funding Agencies (Switzerland); NSC (Taipei); TUBITAK and TAEK (Turkey); STFC (United Kingdom); DOE and NSF (USA). Individuals have received support from the Marie-Curie programme and the European Research Council (European Union); the Leventis Foundation; the A. P. Sloan Foundation; the Alexander von Humboldt Foundation; the Belgian Federal Science Policy Office; the Fonds pour la Formation à la Recherche dans l'Industrie et dans l'Agriculture (FRRIA-Belgium); the Agentschap voor Innovatie door Wetenschap en Technologie (IWT-Belgium); the Council of Science and Industrial Research, India; and the HOMING PLUS programme of Foundation for Polish Science, cofinanced from European Union, Regional Development Fund.

References

- [1] UA1 Collaboration, "Measurement of the bottom quark production cross section in proton-antiproton collisions at $\sqrt{s} = 0.63$ TeV", *Phys. Lett. B* **213** (1988) 405, doi:10.1016/0370-2693(88)91785-6.
- [2] CDF Collaboration, "Measurement of the B Meson Differential Cross Section $d\sigma/dp_T$ in $p\bar{p}$ Collisions at $\sqrt{s} = 1.8$ TeV", *Phys. Rev. Lett.* **75** (1995) 1451, doi:10.1103/PhysRevLett.75.1451.
- [3] CDF Collaboration, "Measurement of the B^+ production cross section in $p\bar{p}$ collisions at $\sqrt{s} = 1960$ GeV", *Phys. Rev. D* **75** (2007) 012010, doi:10.1103/PhysRevD.75.012010.
- [4] D0 Collaboration, "Inclusive μ and b -Quark Production Cross Sections in $p\bar{p}$ Collisions at $\sqrt{s} = 1.8$ TeV", *Phys. Rev. Lett.* **74** (1995) 3548, doi:10.1103/PhysRevLett.74.3548.
- [5] HERA-B Collaboration, "Investigation of heavy-quark production in proton-nucleus collisions with the HERA-B detector", *Phys. Atom. Nucl.* **72** (2009) 675, doi:10.1134/S1063778809040139.

- [6] CMS Collaboration, "Measurement of the B^+ Production Cross Section in pp Collisions at $\sqrt{s} = 7$ TeV", *Phys. Rev. Lett.* **106** (2011) 112001, doi:10.1103/PhysRevLett.106.112001.
- [7] CMS Collaboration, "Measurement of the B^0 Production Cross Section in pp Collisions at $\sqrt{s} = 7$ TeV", *Phys. Rev. Lett.* **106** (2011) 252001, doi:10.1103/PhysRevLett.106.252001.
- [8] CMS Collaboration, "Inclusive b-hadron production cross section with muons in pp collisions at $\sqrt{s} = 7$ TeV", *JHEP* **03** (2011) 090, doi:10.1007/JHEP03(2011)090.
- [9] CMS Collaboration, "Measurement of the B_s^0 Production Cross Section with $B_s^0 \rightarrow J/\psi\phi$ Decays in pp Collisions at $\sqrt{s} = 7$ TeV", *Phys. Rev. D* **84** (2011) 052008, doi:10.1103/PhysRevD.84.052008.
- [10] LHCb Collaboration, "Measurement of $\sigma(pp \rightarrow b\bar{b}X)$ at $\sqrt{s} = 7$ TeV in the forward region", *Phys. Lett. B* **694** (2010) 209, doi:10.1016/j.physletb.2010.10.010.
- [11] CMS Collaboration, "Inclusive b-jet production in pp collisions at $\sqrt{s} = 7$ TeV", *JHEP* **04** (2012) 84, doi:10.1007/JHEP04(2012)084, arXiv:1202.4617.
- [12] ATLAS Collaboration, "Measurement of the inclusive and dijet cross-sections of b-jets in pp collisions at $\sqrt{s} = 7$ TeV with the ATLAS detector", *Eur. Phys. J. C* **71** (2011) 1846, doi:10.1140/epjc/s10052-011-1846-4.
- [13] CMS Collaboration, "Measurement of the cross section for production of $b\bar{b}X$, decaying to muons in pp collisions at $\sqrt{s} = 7$ TeV", (2012). arXiv:1203.3458. Submitted to JHEP.
- [14] P. Nason, S. Dawson, and R. K. Ellis, "The total cross section for the production of heavy quarks in hadronic collisions", *Nucl. Phys. B* **303** (1988) 607, doi:10.1016/0550-3213(88)90422-1.
- [15] M. Cacciari et al., "QCD analysis of first b cross section data at 1.96 TeV", *JHEP* **07** (2004) 033, doi:10.1088/1126-6708/2004/07/033.
- [16] M. Cacciari, M. Greco, and P. Nason, "The p_T spectrum in heavy-flavour hadroproduction", *JHEP* **05** (1998) 007, doi:10.1088/1126-6708/1998/05/007.
- [17] B. A. Kniehl and G. Kramer, "Finite-mass effects on inclusive B-meson hadroproduction", *Phys. Rev. D* **77** (2008) 014011, doi:10.1103/PhysRevD.77.014011.
- [18] CMS Collaboration, "The CMS experiment at the CERN LHC", *JINST* **3** (2008) S08004, doi:10.1088/1748-0221/3/08/S08004.
- [19] S. H. Lee et al., " Λ_c Enhancement from Strongly Coupled Quark-Gluon Plasma", *Phys. Rev. Lett.* **100** (2008) 222301, doi:10.1103/PhysRevLett.100.222301.
- [20] Y. Oh et al., "Heavy baryon/meson ratios in relativistic heavy ion collisions", *Phys. Rev. C* **79** (2009) 044905, doi:10.1103/PhysRevC.79.044905.
- [21] A. Ayala et al., "Heavy flavor nuclear modification factor: more baryons than mesons less energy loss", (2011). arXiv:1110.4587.

- [22] G. H. Arakelyan et al., “Midrapidity Production of Secondaries in pp Collisions at RHIC and LHC Energies in the Quark-Gluon String Model”, *Eur. Phys. J. C* **54** (2008) 577, doi:10.1140/epjc/s10052-008-0554-1.
- [23] C. Merino, C. Pajares, and Y. M. Shabelski, “Particle Production in the Central Region at LHC Energies”, (2011). arXiv:1105.6026.
- [24] Particle Data Group Collaboration, “Review of Particle Physics”, *J. Phys. G* **37** (2010) 075021, doi:10.1088/0954-3899/37/7A/075021.
- [25] CMS Collaboration, “Absolute Calibration of the Luminosity Measurement at CMS: Winter 2012 Update”, CMS Physics Analysis Summary CMS-PAS-SMP-12-008, (2012).
- [26] CMS Collaboration, “CMS tracking performance results from early LHC operation”, *Eur. Phys. J. C* **70** (2010) 1165, doi:10.1140/epjc/s10052-010-1491-3.
- [27] CMS Collaboration, “Performance of muon identification in pp collisions at $\sqrt{s} = 7$ TeV”, CMS Physics Analysis Summary CMS-PAS-MUO-10-002, (2010).
- [28] T. Sjöstrand, S. Mrenna and P. Skands, “PYTHIA 6.4 physics and manual”, *JHEP* **05** (2006) 026, doi:10.1088/1126-6708/2006/05/026.
- [29] D. J. Lange, “The EVTGEN particle decay simulation package”, *Nucl. Instrum. Meth. A* **462** (2001) 152, doi:10.1016/S0168-9002(01)00089-4.
- [30] GEANT4 Collaboration, “GEANT4—a simulation toolkit”, *Nucl. Instrum. Meth. A* **506** (2003) 250, doi:10.1016/S0168-9002(03)01368-8.
- [31] CMS Collaboration, “Prompt and non-prompt J/ψ production in pp collisions at $\sqrt{s} = 7$ TeV”, *Eur. Phys. J. C* **71** (2011) 1575, doi:10.1140/epjc/s10052-011-1575-8.
- [32] CMS Collaboration, “Measurement of Tracking Efficiency”, CMS Physics Analysis Summary CMS-PAS-TRK-10-002, (2010).
- [33] CMS Collaboration, “Strange particle production in pp collisions at $\sqrt{s} = 0.9$ and 7 TeV”, *JHEP* **05** (2011) 064, doi:10.1007/JHEP05(2011)064.
- [34] S. Alioli et al., “A general framework for implementing NLO calculations in shower Monte Carlo programs: the POWHEG BOX”, *JHEP* **06** (2010) 043, doi:10.1007/JHEP06(2010)043.
- [35] S. Frixione, P. Nason, and G. Ridolfi, “A Positive-weight next-to-leading-order Monte Carlo for heavy flavour hadroproduction”, *JHEP* **09** (2007) 126, doi:10.1088/1126-6708/2007/09/126.
- [36] J. Pumplin et al., “New generation of parton distributions with uncertainties from global QCD analysis”, *JHEP* **07** (2002) 012, doi:10.1088/1126-6708/2002/07/012.
- [37] R. Field, “Early LHC Underlying Event Data—Findings and Surprises”, (2010). arXiv:1010.3558. Proceedings of the Hadron Collider Physics Symposium 2010.
- [38] S. Frixione, P. Nason, and B. R. Webber, “Matching NLO QCD and parton showers in heavy flavour production”, *JHEP* **08** (2003) 007, doi:10.1088/1126-6708/2003/08/007.

- [39] DELPHI Collaboration, "Lifetime and production rate of beauty baryons from Z decays", *Z. Phys. C* **68** (1995) 375, doi:10.1007/BF01620730.
- [40] ALEPH Collaboration, "Strange b baryon production and lifetime in Z decays", *Phys. Lett. B* **384** (1996) 449, doi:10.1016/0370-2693(96)00925-2.
- [41] CDF Collaboration, "Measurement of ratios of fragmentation fractions for bottom hadrons in pp collisions at $\sqrt{s} = 1.96$ TeV", *Phys. Rev. D* **77** (2008) 072003, doi:10.1103/PhysRevD.77.072003.
- [42] LHCb Collaboration, "Measurement of b hadron production fractions in 7 TeV pp collisions", *Phys. Rev. D* **85** (2012) 032008, doi:10.1103/PhysRevD.85.032008.
- [43] C. Tsallis, "Possible Generalization of Boltzmann-Gibbs Statistics", *J. Stat. Phys.* **52** (1988) 479, doi:10.1007/BF01016429.
- [44] CMS Collaboration, "Altered scenarios of the CMS Tracker material for systematic uncertainties studies", CMS Note CMS-Note-10-010, (2010).
- [45] ALICE Collaboration, "Midrapidity antiproton-to-proton ratio in pp collisions at $\sqrt{s} = 0.9$ and 7 TeV measured by the ALICE experiment", *Phys. Rev. Lett.* **105** (2010) 072002, doi:10.1103/PhysRevLett.105.072002.

A The CMS Collaboration

Yerevan Physics Institute, Yerevan, Armenia

S. Chatrchyan, V. Khachatryan, A.M. Sirunyan, A. Tumasyan

Institut für Hochenergiephysik der OeAW, Wien, Austria

W. Adam, T. Bergauer, M. Dragicevic, J. Erö, C. Fabjan, M. Friedl, R. Frühwirth, V.M. Ghete, J. Hammer, N. Hörmann, J. Hrubec, M. Jeitler, W. Kiesenhofer, V. Knünz, M. Krammer, D. Liko, I. Mikulec, M. Pernicka[†], B. Rahbaran, C. Rohringer, H. Rohringer, R. Schöfbeck, J. Strauss, A. Taurok, P. Wagner, W. Waltenberger, G. Walzel, E. Widl, C.-E. Wulz

National Centre for Particle and High Energy Physics, Minsk, Belarus

V. Mossolov, N. Shumeiko, J. Suarez Gonzalez

Universiteit Antwerpen, Antwerpen, Belgium

S. Bansal, T. Cornelis, E.A. De Wolf, X. Janssen, S. Luyckx, T. Maes, L. Mucibello, S. Ochesanu, B. Roland, R. Rougny, M. Selvaggi, Z. Staykova, H. Van Haevermaet, P. Van Mechelen, N. Van Remortel, A. Van Spilbeeck

Vrije Universiteit Brussel, Brussel, Belgium

F. Blekman, S. Blyweert, J. D'Hondt, R. Gonzalez Suarez, A. Kalogeropoulos, M. Maes, A. Olbrechts, W. Van Doninck, P. Van Mulders, G.P. Van Onsem, I. Vilella

Université Libre de Bruxelles, Bruxelles, Belgium

O. Charaf, B. Clerbaux, G. De Lentdecker, V. Dero, A.P.R. Gay, T. Hreus, A. Léonard, P.E. Marage, T. Reis, L. Thomas, C. Vander Velde, P. Vanlaer, J. Wang

Ghent University, Ghent, Belgium

V. Adler, K. Bernaert, A. Cimmino, S. Costantini, G. Garcia, M. Grunewald, B. Klein, J. Lellouch, A. Marinov, J. McCartin, A.A. Ocampo Rios, D. Ryckbosch, N. Strobbe, F. Thyssen, M. Tytgat, L. Vanelderen, P. Verwilligen, S. Walsh, E. Yazgan, N. Zaganidis

Université Catholique de Louvain, Louvain-la-Neuve, Belgium

S. Basegmez, G. Bruno, R. Castello, L. Ceard, C. Delaere, T. du Pree, D. Favart, L. Forthomme, A. Giammanco¹, J. Hollar, V. Lemaître, J. Liao, O. Militaru, C. Nuttens, D. Pagano, A. Pin, K. Piotrkowski, N. Schul, J.M. Vizan Garcia

Université de Mons, Mons, Belgium

N. Belyi, T. Caebergs, E. Daubie, G.H. Hammad

Centro Brasileiro de Pesquisas Fisicas, Rio de Janeiro, Brazil

G.A. Alves, M. Correa Martins Junior, D. De Jesus Damiao, T. Martins, M.E. Pol, M.H.G. Souza

Universidade do Estado do Rio de Janeiro, Rio de Janeiro, Brazil

W.L. Aldá Júnior, W. Carvalho, A. Custódio, E.M. Da Costa, C. De Oliveira Martins, S. Fonseca De Souza, D. Matos Figueiredo, L. Mundim, H. Nogima, V. Oguri, W.L. Prado Da Silva, A. Santoro, L. Soares Jorge, A. Sznajder

Instituto de Fisica Teorica, Universidade Estadual Paulista, Sao Paulo, Brazil

C.A. Bernardes², F.A. Dias³, T.R. Fernandez Perez Tomei, E. M. Gregores², C. Lagana, F. Marinho, P.G. Mercadante², S.F. Novaes, Sandra S. Padula

Institute for Nuclear Research and Nuclear Energy, Sofia, Bulgaria

V. Genchev⁴, P. Iaydjiev⁴, S. Piperov, M. Rodozov, S. Stoykova, G. Sultanov, V. Tcholakov, R. Trayanov, M. Vutova

University of Sofia, Sofia, Bulgaria

A. Dimitrov, R. Hadjiiska, V. Kozhuharov, L. Litov, B. Pavlov, P. Petkov

Institute of High Energy Physics, Beijing, China

J.G. Bian, G.M. Chen, H.S. Chen, C.H. Jiang, D. Liang, S. Liang, X. Meng, J. Tao, J. Wang, X. Wang, Z. Wang, H. Xiao, M. Xu, J. Zang, Z. Zhang

State Key Lab. of Nucl. Phys. and Tech., Peking University, Beijing, China

C. Asawatangtrakuldee, Y. Ban, S. Guo, Y. Guo, W. Li, S. Liu, Y. Mao, S.J. Qian, H. Teng, S. Wang, B. Zhu, W. Zou

Universidad de Los Andes, Bogota, Colombia

C. Avila, J.P. Gomez, B. Gomez Moreno, A.F. Osorio Oliveros, J.C. Sanabria

Technical University of Split, Split, Croatia

N. Godinovic, D. Lelas, R. Plestina⁵, D. Polic, I. Puljak⁴

University of Split, Split, Croatia

Z. Antunovic, M. Kovac

Institute Rudjer Boskovic, Zagreb, Croatia

V. Brigljevic, S. Duric, K. Kadija, J. Luetic, S. Morovic

University of Cyprus, Nicosia, Cyprus

A. Attikis, M. Galanti, G. Mavromanolakis, J. Mousa, C. Nicolaou, F. Ptochos, P.A. Razis

Charles University, Prague, Czech Republic

M. Finger, M. Finger Jr.

Academy of Scientific Research and Technology of the Arab Republic of Egypt, Egyptian Network of High Energy Physics, Cairo, Egypt

Y. Assran⁶, S. Elgammal⁷, A. Ellithi Kamel⁸, S. Khalil⁷, M.A. Mahmoud⁹, A. Radi^{10,11}

National Institute of Chemical Physics and Biophysics, Tallinn, Estonia

M. Kadastik, M. Müntel, M. Raidal, L. Rebane, A. Tiko

Department of Physics, University of Helsinki, Helsinki, Finland

V. Azzolini, P. Eerola, G. Fedi, M. Voutilainen

Helsinki Institute of Physics, Helsinki, Finland

J. Härkönen, A. Heikkinen, V. Karimäki, R. Kinnunen, M.J. Kortelainen, T. Lampén, K. Lassila-Perini, S. Lehti, T. Lindén, P. Luukka, T. Mäenpää, T. Peltola, E. Tuominen, J. Tuominiemi, E. Tuovinen, D. Ungaro, L. Wendland

Lappeenranta University of Technology, Lappeenranta, Finland

K. Banzuzi, A. Korpela, T. Tuuva

DSM/IRFU, CEA/Saclay, Gif-sur-Yvette, France

M. Besancon, S. Choudhury, M. Dejardin, D. Denegri, B. Fabbro, J.L. Faure, F. Ferri, S. Ganjour, A. Givernaud, P. Gras, G. Hamel de Monchenault, P. Jarry, E. Locci, J. Malcles, L. Millischer, A. Nayak, J. Rander, A. Rosowsky, I. Shreyber, M. Titov

Laboratoire Leprince-Ringuet, Ecole Polytechnique, IN2P3-CNRS, Palaiseau, France

S. Baffioni, F. Beaudette, L. Benhabib, L. Bianchini, M. Bluj¹², C. Broutin, P. Busson, C. Charlot, N. Daci, T. Dahms, L. Dobrzynski, R. Granier de Cassagnac, M. Haguener, P. Miné, C. Mironov, C. Ochando, P. Paganini, D. Sabes, R. Salerno, Y. Sirois, C. Veelken, A. Zabi

Institut Pluridisciplinaire Hubert Curien, Université de Strasbourg, Université de Haute Alsace Mulhouse, CNRS/IN2P3, Strasbourg, France

J.-L. Agram¹³, J. Andrea, D. Bloch, D. Bodin, J.-M. Brom, M. Cardaci, E.C. Chabert, C. Collard, E. Conte¹³, F. Drouhin¹³, C. Ferro, J.-C. Fontaine¹³, D. Gelé, U. Goerlach, P. Juillot, M. Karim¹³, A.-C. Le Bihan, P. Van Hove

Centre de Calcul de l'Institut National de Physique Nucleaire et de Physique des Particules (IN2P3), Villeurbanne, France

F. Fassi, D. Mercier

Université de Lyon, Université Claude Bernard Lyon 1, CNRS-IN2P3, Institut de Physique Nucléaire de Lyon, Villeurbanne, France

S. Beauceron, N. Beaupere, O. Bondu, G. Boudoul, H. Brun, J. Chasserat, R. Chierici⁴, D. Contardo, P. Depasse, H. El Mamouni, J. Fay, S. Gascon, M. Gouzevitch, B. Ille, T. Kurca, M. Lethuillier, L. Mirabito, S. Perries, V. Sordini, S. Tosi, Y. Tschudi, P. Verdier, S. Viret

Institute of High Energy Physics and Informatization, Tbilisi State University, Tbilisi, Georgia

Z. Tsamalaidze¹⁴

RWTH Aachen University, I. Physikalisches Institut, Aachen, Germany

G. Anagnostou, S. Beranek, M. Edelhoff, L. Feld, N. Heracleous, O. Hindrichs, R. Jussen, K. Klein, J. Merz, A. Ostapchuk, A. Perieanu, F. Raupach, J. Sammet, S. Schael, D. Sprenger, H. Weber, B. Wittmer, V. Zhukov¹⁵

RWTH Aachen University, III. Physikalisches Institut A, Aachen, Germany

M. Ata, J. Caudron, E. Dietz-Laursonn, M. Erdmann, A. Güth, T. Hebbeker, C. Heidemann, K. Hoepfner, D. Klingebiel, P. Kreuzer, J. Lingemann, C. Magass, M. Merschmeyer, A. Meyer, M. Olschewski, P. Papacz, H. Pieta, H. Reithler, S.A. Schmitz, L. Sonnenschein, J. Steggemann, D. Teyssier, M. Weber

RWTH Aachen University, III. Physikalisches Institut B, Aachen, Germany

M. Bontenackels, V. Cherepanov, M. Davids, G. Flügge, H. Geenen, M. Geisler, W. Haj Ahmad, F. Hoehle, B. Kargoll, T. Kress, Y. Kuessel, A. Linn, A. Nowack, L. Perchalla, O. Pooth, J. Rennefeld, P. Sauerland, A. Stahl

Deutsches Elektronen-Synchrotron, Hamburg, Germany

M. Aldaya Martin, J. Behr, W. Behrenhoff, U. Behrens, M. Bergholz¹⁶, A. Bethani, K. Borras, A. Burgmeier, A. Cakir, L. Calligaris, A. Campbell, E. Castro, F. Costanza, D. Dammann, G. Eckerlin, D. Eckstein, D. Fischer, G. Flucke, A. Geiser, I. Glushkov, S. Habib, J. Hauk, H. Jung⁴, M. Kasemann, P. Katsas, C. Kleinwort, H. Kluge, A. Knutsson, M. Krämer, D. Krücker, E. Kuznetsova, W. Lange, W. Lohmann¹⁶, B. Lutz, R. Mankel, I. Marfin, M. Marienfeld, I.-A. Melzer-Pellmann, A.B. Meyer, J. Mnich, A. Mussgiller, S. Naumann-Emme, J. Olzem, H. Perrey, A. Petrukhin, D. Pitzl, A. Raspereza, P.M. Ribeiro Cipriano, C. Riedl, M. Rosin, J. Salfeld-Nebgen, R. Schmidt¹⁶, T. Schoerner-Sadenius, N. Sen, A. Spiridonov, M. Stein, R. Walsh, C. Wissing

University of Hamburg, Hamburg, Germany

C. Autermann, V. Blobel, S. Bobrovskiy, J. Draeger, H. Enderle, J. Erfle, U. Gebbert, M. Görner, T. Hermanns, R.S. Höing, K. Kaschube, G. Kaussen, H. Kirschenmann, R. Klanner, J. Lange, B. Mura, F. Nowak, T. Peiffer, N. Pietsch, C. Sander, H. Schettler, P. Schleper, E. Schlieckau, A. Schmidt, M. Schröder, T. Schum, H. Stadie, G. Steinbrück, J. Thomsen

Institut für Experimentelle Kernphysik, Karlsruhe, Germany

C. Barth, J. Berger, T. Chwalek, W. De Boer, A. Dierlamm, M. Feindt, M. Guthoff⁴, C. Hackstein, F. Hartmann, M. Heinrich, H. Held, K.H. Hoffmann, S. Honc, I. Katkov¹⁵, J.R. Komaragiri, D. Martschei, S. Mueller, Th. Müller, M. Niegel, A. Nürnberg, O. Oberst, A. Oehler, J. Ott, G. Quast, K. Rabbertz, F. Ratnikov, N. Ratnikova, S. Röcker, A. Scheurer, F.-P. Schilling, G. Schott, H.J. Simonis, F.M. Stober, D. Troendle, R. Ulrich, J. Wagner-Kuhr, T. Weiler, M. Zeise

Institute of Nuclear Physics "Demokritos", Aghia Paraskevi, Greece

G. Daskalakis, T. Geralis, S. Kesisoglou, A. Kyriakis, D. Loukas, I. Manolakos, A. Markou, C. Markou, C. Mavrommatis, E. Ntomari

University of Athens, Athens, Greece

L. Gouskos, T.J. Mertzimekis, A. Panagiotou, N. Saoulidou

University of Ioánnina, Ioánnina, Greece

I. Evangelou, C. Foudas⁴, P. Kokkas, N. Manthos, I. Papadopoulos, V. Patras

KFKI Research Institute for Particle and Nuclear Physics, Budapest, Hungary

G. Bencze, C. Hajdu⁴, P. Hidas, D. Horvath¹⁷, K. Krajczar¹⁸, B. Radics, F. Sikler⁴, V. Veszpremi, G. Vesztergombi¹⁸

Institute of Nuclear Research ATOMKI, Debrecen, Hungary

N. Beni, S. Czellar, J. Molnar, J. Palinkas, Z. Szillasi

University of Debrecen, Debrecen, Hungary

J. Karancsi, P. Raics, Z.L. Trocsanyi, B. Ujvari

Panjab University, Chandigarh, India

S.B. Beri, V. Bhatnagar, N. Dhingra, R. Gupta, M. Jindal, M. Kaur, J.M. Kohli, M.Z. Mehta, N. Nishu, L.K. Saini, A. Sharma, J. Singh

University of Delhi, Delhi, India

S. Ahuja, A. Bhardwaj, B.C. Choudhary, A. Kumar, A. Kumar, S. Malhotra, M. Naimuddin, K. Ranjan, V. Sharma, R.K. Shivpuri

Saha Institute of Nuclear Physics, Kolkata, India

S. Banerjee, S. Bhattacharya, S. Dutta, B. Gomber, Sa. Jain, Sh. Jain, R. Khurana, S. Sarkar, M. Sharan

Bhabha Atomic Research Centre, Mumbai, India

A. Abdulsalam, R.K. Choudhury, D. Dutta, S. Kailas, V. Kumar, P. Mehta, A.K. Mohanty⁴, L.M. Pant, P. Shukla

Tata Institute of Fundamental Research - EHEP, Mumbai, India

T. Aziz, S. Ganguly, M. Guchait¹⁹, M. Maity²⁰, G. Majumder, K. Mazumdar, G.B. Mohanty, B. Parida, K. Sudhakar, N. Wickramage

Tata Institute of Fundamental Research - HECR, Mumbai, India

S. Banerjee, S. Dugad

Institute for Research in Fundamental Sciences (IPM), Tehran, Iran

H. Arfaei, H. Bakhshiansohi²¹, S.M. Etesami²², A. Fahim²¹, M. Hashemi, H. Hesari, A. Jafari²¹, M. Khakzad, A. Mohammadi²³, M. Mohammadi Najafabadi, S. Paktinat Mehdiabadi, B. Safarzadeh²⁴, M. Zeinali²²

INFN Sezione di Bari ^a, Università di Bari ^b, Politecnico di Bari ^c, Bari, Italy

M. Abbrescia^{a,b}, L. Barbone^{a,b}, C. Calabria^{a,b,4}, S.S. Chhibra^{a,b}, A. Colaleo^a, D. Creanza^{a,c}, N. De Filippis^{a,c,4}, M. De Palma^{a,b}, L. Fiore^a, G. Iaselli^{a,c}, L. Lusito^{a,b}, G. Maggi^{a,c}, M. Maggi^a, B. Marangelli^{a,b}, S. My^{a,c}, S. Nuzzo^{a,b}, N. Pacifico^{a,b}, A. Pompili^{a,b}, G. Pugliese^{a,c}, G. Selvaggi^{a,b}, L. Silvestris^a, G. Singh^{a,b}, G. Zito^a

INFN Sezione di Bologna ^a, Università di Bologna ^b, Bologna, Italy

G. Abbiendi^a, A.C. Benvenuti^a, D. Bonacorsi^{a,b}, S. Braibant-Giacomelli^{a,b}, L. Brigliadori^{a,b}, P. Capiluppi^{a,b}, A. Castro^{a,b}, F.R. Cavallo^a, M. Cuffiani^{a,b}, G.M. Dallavalle^a, F. Fabbri^a, A. Fanfani^{a,b}, D. Fasanella^{a,b,4}, P. Giacomelli^a, C. Grandi^a, L. Guiducci, S. Marcellini^a, G. Masetti^a, M. Meneghelli^{a,b,4}, A. Montanari^a, F.L. Navarria^{a,b}, F. Odorici^a, A. Perrotta^a, F. Primavera^{a,b}, A.M. Rossi^{a,b}, T. Rovelli^{a,b}, G. Siroli^{a,b}, R. Travaglini^{a,b}

INFN Sezione di Catania ^a, Università di Catania ^b, Catania, Italy

S. Albergo^{a,b}, G. Cappello^{a,b}, M. Chiorboli^{a,b}, S. Costa^{a,b}, R. Potenza^{a,b}, A. Tricomi^{a,b}, C. Tuve^{a,b}

INFN Sezione di Firenze ^a, Università di Firenze ^b, Firenze, Italy

G. Barbagli^a, V. Ciulli^{a,b}, C. Civinini^a, R. D'Alessandro^{a,b}, E. Focardi^{a,b}, S. Frosali^{a,b}, E. Gallo^a, S. Gonzi^{a,b}, M. Meschini^a, S. Paoletti^a, G. Sguazzoni^a, A. Tropiano^{a,4}

INFN Laboratori Nazionali di Frascati, Frascati, Italy

L. Benussi, S. Bianco, S. Colafranceschi²⁵, F. Fabbri, D. Piccolo

INFN Sezione di Genova, Genova, Italy

P. Fabbriatore, R. Musenich

INFN Sezione di Milano-Bicocca ^a, Università di Milano-Bicocca ^b, Milano, Italy

A. Benaglia^{a,b,4}, F. De Guio^{a,b}, L. Di Matteo^{a,b,4}, S. Fiorendi^{a,b}, S. Gennai^{a,4}, A. Ghezzi^{a,b}, S. Malvezzi^a, R.A. Manzoni^{a,b}, A. Martelli^{a,b}, A. Massironi^{a,b,4}, D. Menasce^a, L. Moroni^a, M. Paganoni^{a,b}, D. Pedrini^a, S. Ragazzi^{a,b}, N. Redaelli^a, S. Sala^a, T. Tabarelli de Fatis^{a,b}

INFN Sezione di Napoli ^a, Università di Napoli "Federico II" ^b, Napoli, Italy

S. Buontempo^a, C.A. Carrillo Montoya^{a,4}, N. Cavallo^{a,26}, A. De Cosa^{a,b,4}, O. Dogangun^{a,b}, F. Fabozzi^{a,26}, A.O.M. Iorio^{a,4}, L. Lista^a, S. Meola^{a,27}, M. Merola^{a,b}, P. Paolucci^{a,4}

INFN Sezione di Padova ^a, Università di Padova ^b, Università di Trento (Trento) ^c, Padova, Italy

P. Azzi^a, N. Bacchetta^{a,4}, P. Bellan^{a,b}, D. Bisello^{a,b}, A. Branca^{a,4}, R. Carlin^{a,b}, P. Checchia^a, T. Dorigo^a, U. Dosselli^a, F. Gasparini^{a,b}, A. Gozzelino^a, K. Kanishchev^{a,c}, S. Lacaprara^a, I. Lazzizzera^{a,c}, M. Margoni^{a,b}, A.T. Meneguzzo^{a,b}, M. Nespolo^{a,4}, L. Perrozzi^a, N. Pozzobon^{a,b}, P. Ronchese^{a,b}, F. Simonetto^{a,b}, E. Torassa^a, M. Tosi^{a,b,4}, S. Vanini^{a,b}, P. Zotto^{a,b}

INFN Sezione di Pavia ^a, Università di Pavia ^b, Pavia, Italy

M. Gabusi^{a,b}, S.P. Ratti^{a,b}, C. Riccardi^{a,b}, P. Torre^{a,b}, P. Vitulo^{a,b}

INFN Sezione di Perugia ^a, Università di Perugia ^b, Perugia, Italy

M. Biasini^{a,b}, G.M. Bilei^a, L. Fanò^{a,b}, P. Lariccia^{a,b}, A. Lucaroni^{a,b,4}, G. Mantovani^{a,b}, M. Menichelli^a, A. Nappi^{a,b}, F. Romeo^{a,b}, A. Saha, A. Santocchia^{a,b}, S. Taroni^{a,b,4}

INFN Sezione di Pisa ^a, Università di Pisa ^b, Scuola Normale Superiore di Pisa ^c, Pisa, Italy

P. Azzurri^{a,c}, G. Bagliesi^a, T. Boccali^a, G. Broccolo^{a,c}, R. Castaldi^a, R.T. D'Agnolo^{a,c}, R. Dell'Orso^a, F. Fiori^{a,b,4}, L. Foà^{a,c}, A. Giassi^a, A. Kraan^a, F. Ligabue^{a,c}, T. Lomtadze^a, L. Martini^{a,28}, A. Messineo^{a,b}, F. Palla^a, F. Palmonari^a, A. Rizzi^{a,b}, A.T. Serban^{a,29}, P. Spagnolo^a, P. Squillacioti^{a,4}, R. Tenchini^a, G. Tonelli^{a,b,4}, A. Venturi^{a,4}, P.G. Verdini^a

INFN Sezione di Roma ^a, Università di Roma "La Sapienza" ^b, Roma, Italy

L. Barone^{a,b}, F. Cavallari^a, D. Del Re^{a,b,4}, M. Diemoz^a, M. Grassi^{a,b,4}, E. Longo^{a,b}, P. Meridiani^{a,4}, F. Micheli^{a,b}, S. Nourbakhsh^{a,b}, G. Organtini^{a,b}, R. Paramatti^a, S. Rahatlou^{a,b}, M. Sigamani^a, L. Soffi^{a,b}

INFN Sezione di Torino ^a, Università di Torino ^b, Università del Piemonte Orientale (Novara) ^c, Torino, Italy

N. Amapane^{a,b}, R. Arcidiacono^{a,c}, S. Argiro^{a,b}, M. Arneodo^{a,c}, C. Biino^a, C. Botta^{a,b}, N. Cartiglia^a, M. Costa^{a,b}, P. De Remigis^a, N. Demaria^a, A. Graziano^{a,b}, C. Mariotti^{a,4}, S. Maselli^a, E. Migliore^{a,b}, V. Monaco^{a,b}, M. Musich^{a,4}, M.M. Obertino^{a,c}, N. Pastrone^a, M. Pelliccioni^a, A. Potenza^{a,b}, A. Romero^{a,b}, M. Ruspa^{a,c}, R. Sacchi^{a,b}, A. Solano^{a,b}, A. Staiano^a, A. Vilela Pereira^a

INFN Sezione di Trieste ^a, Università di Trieste ^b, Trieste, Italy

S. Belforte^a, F. Cossutti^a, G. Della Ricca^{a,b}, B. Gobbo^a, M. Marone^{a,b,4}, D. Montanino^{a,b,4}, A. Penzo^a, A. Schizzi^{a,b}

Kangwon National University, Chunchon, Korea

S.G. Heo, T.Y. Kim, S.K. Nam

Kyungpook National University, Daegu, Korea

S. Chang, J. Chung, D.H. Kim, G.N. Kim, D.J. Kong, H. Park, S.R. Ro, D.C. Son, T. Son

Chonnam National University, Institute for Universe and Elementary Particles, Kwangju, Korea

J.Y. Kim, Zero J. Kim, S. Song

Konkuk University, Seoul, Korea

H.Y. Jo

Korea University, Seoul, Korea

S. Choi, D. Gyun, B. Hong, M. Jo, H. Kim, T.J. Kim, K.S. Lee, D.H. Moon, S.K. Park, E. Seo

University of Seoul, Seoul, Korea

M. Choi, S. Kang, H. Kim, J.H. Kim, C. Park, I.C. Park, S. Park, G. Ryu

Sungkyunkwan University, Suwon, Korea

Y. Cho, Y. Choi, Y.K. Choi, J. Goh, M.S. Kim, E. Kwon, B. Lee, J. Lee, S. Lee, H. Seo, I. Yu

Vilnius University, Vilnius, Lithuania

M.J. Bilinskas, I. Grigelionis, M. Janulis, A. Juodagalvis

Centro de Investigacion y de Estudios Avanzados del IPN, Mexico City, Mexico

H. Castilla-Valdez, E. De La Cruz-Burelo, I. Heredia-de La Cruz, R. Lopez-Fernandez, R. Magaña Villalba, J. Martínez-Ortega, A. Sánchez-Hernández, L.M. Villasenor-Cendejas

Universidad Iberoamericana, Mexico City, Mexico

S. Carrillo Moreno, F. Vazquez Valencia

Benemerita Universidad Autonoma de Puebla, Puebla, Mexico

H.A. Salazar Ibarguen

Universidad Autónoma de San Luis Potosí, San Luis Potosí, Mexico

E. Casimiro Linares, A. Morelos Pineda, M.A. Reyes-Santos

University of Auckland, Auckland, New Zealand

D. Krofcheck

University of Canterbury, Christchurch, New Zealand

A.J. Bell, P.H. Butler, R. Doesburg, S. Reucroft, H. Silverwood

National Centre for Physics, Quaid-I-Azam University, Islamabad, Pakistan

M. Ahmad, M.I. Asghar, H.R. Hoorani, S. Khalid, W.A. Khan, T. Khurshid, S. Qazi, M.A. Shah, M. Shoaib

Institute of Experimental Physics, Faculty of Physics, University of Warsaw, Warsaw, Poland

G. Brona, K. Bunkowski, M. Cwiok, W. Dominik, K. Doroba, A. Kalinowski, M. Konecki, J. Krolikowski

Soltan Institute for Nuclear Studies, Warsaw, Poland

H. Bialkowska, B. Boimska, T. Frueboes, R. Gokieli, M. Górski, M. Kazana, K. Nawrocki, K. Romanowska-Rybinska, M. Szleper, G. Wrochna, P. Zalewski

Laboratório de Instrumentação e Física Experimental de Partículas, Lisboa, Portugal

N. Almeida, P. Bargassa, A. David, P. Faccioli, P.G. Ferreira Parracho, M. Gallinaro, J. Seixas, J. Varela, P. Vischia

Joint Institute for Nuclear Research, Dubna, Russia

I. Belotelov, P. Bunin, M. Gavrilenko, I. Golutvin, I. Gorbunov, A. Kamenev, V. Karjavin, G. Kozlov, A. Lanev, A. Malakhov, P. Moisezenz, V. Palichik, V. Pereygin, S. Shmatov, V. Smirnov, A. Volodko, A. Zarubin

Petersburg Nuclear Physics Institute, Gatchina (St Petersburg), Russia

S. Evstyukhin, V. Golovtsov, Y. Ivanov, V. Kim, P. Levchenko, V. Murzin, V. Oreshkin, I. Smirnov, V. Sulimov, L. Uvarov, S. Vavilov, A. Vorobyev, An. Vorobyev

Institute for Nuclear Research, Moscow, Russia

Yu. Andreev, A. Dermenev, S. Gninenko, N. Golubev, M. Kirsanov, N. Krasnikov, V. Matveev, A. Pashenkov, D. Tlisov, A. Toropin

Institute for Theoretical and Experimental Physics, Moscow, Russia

V. Epshteyn, M. Erofeeva, V. Gavrilov, M. Kossov⁴, N. Lychkovskaya, V. Popov, G. Safronov, S. Semenov, V. Stolin, E. Vlasov, A. Zhokin

Moscow State University, Moscow, Russia

A. Belyaev, E. Boos, M. Dubinin³, L. Dudko, A. Ershov, A. Gribushin, V. Klyukhin, O. Kodolova, I. Lokhtin, A. Markina, S. Obraztsov, M. Perfilov, S. Petrushanko, A. Popov, L. Sarycheva[†], V. Savrin, A. Snigirev

P.N. Lebedev Physical Institute, Moscow, Russia

V. Andreev, M. Azarkin, I. Dremin, M. Kirakosyan, A. Leonidov, G. Mesyats, S.V. Rusakov, A. Vinogradov

State Research Center of Russian Federation, Institute for High Energy Physics, Protvino, Russia

I. Azhgirey, I. Bayshev, S. Bitioukov, V. Grishin⁴, V. Kachanov, D. Konstantinov, A. Korablev, V. Krychkin, V. Petrov, R. Ryutin, A. Sobol, L. Tourtchanovitch, S. Troshin, N. Tyurin, A. Uzunian, A. Volkov

University of Belgrade, Faculty of Physics and Vinca Institute of Nuclear Sciences, Belgrade, Serbia

P. Adzic³⁰, M. Djordjevic, M. Ekmedzic, D. Krpic³⁰, J. Milosevic

Centro de Investigaciones Energéticas Medioambientales y Tecnológicas (CIEMAT), Madrid, Spain

M. Aguilar-Benitez, J. Alcaraz Maestre, P. Arce, C. Battilana, E. Calvo, M. Cerrada, M. Chamizo Llatas, N. Colino, B. De La Cruz, A. Delgado Peris, C. Diez Pardos, D. Domínguez Vázquez, C. Fernandez Bedoya, J.P. Fernández Ramos, A. Ferrando, J. Flix, M.C. Fouz, P. Garcia-Abia, O. Gonzalez Lopez, S. Goy Lopez, J.M. Hernandez, M.I. Josa, G. Merino, J. Puerta Pelayo, A. Quintario Olmeda, I. Redondo, L. Romero, J. Santaolalla, M.S. Soares, C. Willmott

Universidad Autónoma de Madrid, Madrid, Spain

C. Albajar, G. Codispoti, J.F. de Trocóniz

Universidad de Oviedo, Oviedo, Spain

J. Cuevas, J. Fernandez Menendez, S. Folgueras, I. Gonzalez Caballero, L. Lloret Iglesias, J. Piedra Gomez³¹

Instituto de Física de Cantabria (IFCA), CSIC-Universidad de Cantabria, Santander, Spain

J.A. Brochero Cifuentes, I.J. Cabrillo, A. Calderon, S.H. Chuang, J. Duarte Campderros, M. Felcini³², M. Fernandez, G. Gomez, J. Gonzalez Sanchez, C. Jorda, P. Lobelle Pardo, A. Lopez Virto, J. Marco, R. Marco, C. Martinez Rivero, F. Matorras, F.J. Munoz Sanchez, T. Rodrigo, A.Y. Rodríguez-Marrero, A. Ruiz-Jimeno, L. Scodellaro, M. Sobron Sanudo, I. Vila, R. Vilar Cortabitarte

CERN, European Organization for Nuclear Research, Geneva, Switzerland

D. Abbaneo, E. Auffray, G. Auzinger, P. Baillon, A.H. Ball, D. Barney, C. Bernet⁵, G. Bianchi, P. Bloch, A. Bocci, A. Bonato, H. Breuker, T. Camporesi, G. Cerminara, T. Christiansen, J.A. Coarasa Perez, D. D'Enterria, A. Dabrowski, A. De Roeck, S. Di Guida, M. Dobson, N. Dupont-Sagorin, A. Elliott-Peisert, B. Frisch, W. Funk, G. Georgiou, M. Giffels, D. Gigi, K. Gill, D. Giordano, M. Giunta, F. Glege, R. Gomez-Reino Garrido, P. Govoni, S. Gowdy, R. Guida, M. Hansen, P. Harris, C. Hartl, J. Harvey, B. Hegner, A. Hinzmann, V. Innocente, P. Janot, K. Kaadze, E. Karavakis, K. Kousouris, P. Lecoq, Y.-J. Lee, P. Lenzi, C. Lourenço, T. Mäki, M. Malberti, L. Malgeri, M. Mannelli, L. Masetti, F. Meijers, S. Mersi, E. Meschi, R. Moser, M.U. Mozer, M. Mulders, P. Musella, E. Nesvold, M. Nguyen, T. Orimoto, L. Orsini, E. Palencia Cortezon, E. Perez, A. Petrilli, A. Pfeiffer, M. Pierini, M. Pimiä, D. Piparo, G. Polese, L. Quertenmont, A. Racz, W. Reece, J. Rodrigues Antunes, G. Rolandi³³, T. Rommerskirchen, C. Rovelli³⁴, M. Rovere, H. Sakulin, F. Santanastasio, C. Schäfer, C. Schwick, I. Segoni, S. Sekmen, A. Sharma, P. Siegrist, P. Silva, M. Simon, P. Sphicas³⁵, D. Spiga, M. Spiropulu³, M. Stoye, A. Tsirou, G.I. Veres¹⁸, J.R. Vlimant, H.K. Wöhri, S.D. Worm³⁶, W.D. Zeuner

Paul Scherrer Institut, Villigen, Switzerland

W. Bertl, K. Deiters, W. Erdmann, K. Gabathuler, R. Horisberger, Q. Ingram, H.C. Kaestli, S. König, D. Kotlinski, U. Langenegger, F. Meier, D. Renker, T. Rohe, J. Sibille³⁷

Institute for Particle Physics, ETH Zurich, Zurich, Switzerland

L. Bäni, P. Bortignon, M.A. Buchmann, B. Casal, N. Chanon, Z. Chen, A. Deisher, G. Dissertori, M. Dittmar, M. Dünser, J. Eugster, K. Freudenreich, C. Grab, D. Hits, P. Lecomte, W. Lustermann, P. Martinez Ruiz del Arbol, N. Mohr, F. Moortgat, C. Nägeli³⁸, P. Nef, F. Nessi-Tedaldi, F. Pandolfi, L. Pape, F. Pauss, M. Peruzzi, F.J. Ronga, M. Rossini, L. Sala, A.K. Sanchez, A. Starodumov³⁹, B. Stieger, M. Takahashi, L. Tauscher[†], A. Thea, K. Theofilatos, D. Treille, C. Urscheler, R. Wallny, H.A. Weber, L. Wehrli

Universität Zürich, Zurich, Switzerland

E. Aguilo, C. AMSler, V. Chiochia, S. De Visscher, C. Favaro, M. Ivova Rikova, B. Millan Mejias, P. Otiougova, P. Robmann, H. Snoek, S. Tupputi, M. Verzetti

National Central University, Chung-Li, Taiwan

Y.H. Chang, K.H. Chen, C.M. Kuo, S.W. Li, W. Lin, Z.K. Liu, Y.J. Lu, D. Mekterovic, A.P. Singh, R. Volpe, S.S. Yu

National Taiwan University (NTU), Taipei, Taiwan

P. Bartalini, P. Chang, Y.H. Chang, Y.W. Chang, Y. Chao, K.F. Chen, C. Dietz, U. Grundler, W.-S. Hou, Y. Hsiung, K.Y. Kao, Y.J. Lei, R.-S. Lu, D. Majumder, E. Petrakou, X. Shi, J.G. Shiu, Y.M. Tzeng, X. Wan, M. Wang

Cukurova University, Adana, Turkey

A. Adiguzel, M.N. Bakirci⁴⁰, S. Cerci⁴¹, C. Dozen, I. Dumanoglu, E. Eskut, S. Girgis, G. Gokbulut, E. Gurpinar, I. Hos, E.E. Kangal, G. Karapinar, A. Kayis Topaksu, G. Onengut, K. Ozdemir, S. Ozturk⁴², A. Polatoz, K. Sogut⁴³, D. Sunar Cerci⁴¹, B. Tali⁴¹, H. Topakli⁴⁰, L.N. Vergili, M. Vergili

Middle East Technical University, Physics Department, Ankara, Turkey

I.V. Akin, T. Aliev, B. Bilin, S. Bilmis, M. Deniz, H. Gamsizkan, A.M. Guler, K. Ocalan, A. Ozpineci, M. Serin, R. Sever, U.E. Surat, M. Yalvac, E. Yildirim, M. Zeyrek

Bogazici University, Istanbul, Turkey

E. Gülmez, B. Isildak⁴⁴, M. Kaya⁴⁵, O. Kaya⁴⁵, S. Ozkorucuklu⁴⁶, N. Sonmez⁴⁷

Istanbul Technical University, Istanbul, Turkey

K. Cankocak

National Scientific Center, Kharkov Institute of Physics and Technology, Kharkov, Ukraine

L. Levchuk

University of Bristol, Bristol, United Kingdom

F. Bostock, J.J. Brooke, E. Clement, D. Cussans, H. Flacher, R. Frazier, J. Goldstein, M. Grimes, G.P. Heath, H.F. Heath, L. Kreczko, S. Metson, D.M. Newbold³⁶, K. Nirunpong, A. Poll, S. Senkin, V.J. Smith, T. Williams

Rutherford Appleton Laboratory, Didcot, United Kingdom

L. Basso⁴⁸, K.W. Bell, A. Belyaev⁴⁸, C. Brew, R.M. Brown, D.J.A. Cockerill, J.A. Coughlan, K. Harder, S. Harper, J. Jackson, B.W. Kennedy, E. Olaiya, D. Petyt, B.C. Radburn-Smith, C.H. Shepherd-Themistocleous, I.R. Tomalin, W.J. Womersley

Imperial College, London, United Kingdom

R. Bainbridge, G. Ball, R. Beuselinck, O. Buchmuller, D. Colling, N. Cripps, M. Cutajar, P. Dauncey, G. Davies, M. Della Negra, W. Ferguson, J. Fulcher, D. Futyan, A. Gilbert, A. Guneratne Bryer, G. Hall, Z. Hatherell, J. Hays, G. Iles, M. Jarvis, G. Karapostoli, L. Lyons, A.-M. Magnan, J. Marrouche, B. Mathias, R. Nandi, J. Nash, A. Nikitenko³⁹, A. Papageorgiou, J. Pela⁴, M. Pesaresi, K. Petridis, M. Pioppi⁴⁹, D.M. Raymond, S. Rogerson, A. Rose, M.J. Ryan, C. Seez, P. Sharp[†], A. Sparrow, A. Tapper, M. Vazquez Acosta, T. Virdee, S. Wakefield, N. Wardle, T. Whyntie

Brunel University, Uxbridge, United Kingdom

M. Chadwick, J.E. Cole, P.R. Hobson, A. Khan, P. Kyberd, D. Leslie, W. Martin, I.D. Reid, P. Symonds, L. Teodorescu, M. Turner

Baylor University, Waco, USA

K. Hatakeyama, H. Liu, T. Scarborough

The University of Alabama, Tuscaloosa, USA

C. Henderson, P. Rumerio

Boston University, Boston, USA

A. Avetisyan, T. Bose, C. Fantasia, A. Heister, J. St. John, P. Lawson, D. Lazic, J. Rohlf, D. Sperka, L. Sulak

Brown University, Providence, USA

J. Alimena, S. Bhattacharya, D. Cutts, A. Ferapontov, U. Heintz, S. Jabeen, G. Kukartsev, G. Landsberg, M. Luk, M. Narain, D. Nguyen, M. Segala, T. Sinthuprasith, T. Speer, K.V. Tsang

University of California, Davis, Davis, USA

R. Breedon, G. Breto, M. Calderon De La Barca Sanchez, S. Chauhan, M. Chertok, J. Conway, R. Conway, P.T. Cox, J. Dolen, R. Erbacher, M. Gardner, R. Houtz, W. Ko, A. Kopecky, R. Lander, O. Mall, T. Miceli, R. Nelson, D. Pellett, B. Rutherford, M. Searle, J. Smith, M. Squires, M. Tripathi, R. Vasquez Sierra

University of California, Los Angeles, Los Angeles, USA

V. Andreev, D. Cline, R. Cousins, J. Duris, S. Erhan, P. Everaerts, C. Farrell, J. Hauser, M. Ignatenko, C. Plager, G. Rakness, P. Schlein[†], J. Tucker, V. Valuev, M. Weber

University of California, Riverside, Riverside, USA

J. Babb, R. Clare, M.E. Dinardo, J. Ellison, J.W. Gary, F. Giordano, G. Hanson, G.Y. Jeng⁵⁰, H. Liu, O.R. Long, A. Luthra, H. Nguyen, S. Paramesvaran, J. Sturdy, S. Sumowidagdo, R. Wilken, S. Wimpenny

University of California, San Diego, La Jolla, USA

W. Andrews, J.G. Branson, G.B. Cerati, S. Cittolin, D. Evans, F. Golf, A. Holzner, R. Kelley, M. Lebourgeois, J. Letts, I. Macneill, B. Mangano, S. Padhi, C. Palmer, G. Petrucciani, M. Pieri, M. Sani, V. Sharma, S. Simon, E. Sudano, M. Tadel, Y. Tu, A. Vartak, S. Wasserbaech⁵¹, F. Würthwein, A. Yagil, J. Yoo

University of California, Santa Barbara, Santa Barbara, USA

D. Barge, R. Bellan, C. Campagnari, M. D'Alfonso, T. Danielson, K. Flowers, P. Geffert, J. Incandela, C. Justus, P. Kalavase, S.A. Koay, D. Kovalskyi, V. Krutelyov, S. Lowette, N. Mccoll, V. Pavlunin, F. Rebassoo, J. Ribnik, J. Richman, R. Rossin, D. Stuart, W. To, C. West

California Institute of Technology, Pasadena, USA

A. Apresyan, A. Bornheim, Y. Chen, E. Di Marco, J. Duarte, M. Gataullin, Y. Ma, A. Mott, H.B. Newman, C. Rogan, V. Timciuc, P. Traczyk, J. Veverka, R. Wilkinson, Y. Yang, R.Y. Zhu

Carnegie Mellon University, Pittsburgh, USA

B. Akgun, R. Carroll, T. Ferguson, Y. Iiyama, D.W. Jang, Y.F. Liu, M. Paulini, H. Vogel, I. Vorobiev

University of Colorado at Boulder, Boulder, USA

J.P. Cumalat, B.R. Drell, C.J. Edelmaier, W.T. Ford, A. Gaz, B. Heyburn, E. Luiggi Lopez, J.G. Smith, K. Stenson, K.A. Ulmer, S.R. Wagner

Cornell University, Ithaca, USA

L. Agostino, J. Alexander, A. Chatterjee, N. Eggert, L.K. Gibbons, B. Heltsley, W. Hopkins, A. Khukhunaishvili, B. Kreis, N. Mirman, G. Nicolas Kaufman, J.R. Patterson, A. Ryd, E. Salvati, W. Sun, W.D. Teo, J. Thom, J. Thompson, J. Vaughan, Y. Weng, L. Winstrom, P. Wittich

Fairfield University, Fairfield, USA

D. Winn

Fermi National Accelerator Laboratory, Batavia, USA

S. Abdullin, M. Albrow, J. Anderson, L.A.T. Bauerdick, A. Beretvas, J. Berryhill, P.C. Bhat, I. Bloch, K. Burkett, J.N. Butler, V. Chetluru, H.W.K. Cheung, F. Chlebana, V.D. Elvira, I. Fisk, J. Freeman, Y. Gao, D. Green, O. Gutsche, A. Hahn, J. Hanlon, R.M. Harris, J. Hirschauer, B. Hooberman, S. Jindariani, M. Johnson, U. Joshi, B. Kilminster, B. Klima, S. Kunori, S. Kwan, C. Leonidopoulos, D. Lincoln, R. Lipton, L. Lueking, J. Lykken, K. Maeshima, J.M. Marraffino, S. Maruyama, D. Mason, P. McBride, K. Mishra, S. Mrenna, Y. Musienko⁵², C. Newman-Holmes, V. O'Dell, O. Prokofyev, E. Sexton-Kennedy, S. Sharma, W.J. Spalding, L. Spiegel, P. Tan, L. Taylor, S. Tkaczyk, N.V. Tran, L. Uplegger, E.W. Vaandering, R. Vidal, J. Whitmore, W. Wu, F. Yang, F. Yumiceva, J.C. Yun

University of Florida, Gainesville, USA

D. Acosta, P. Avery, D. Bourilkov, M. Chen, S. Das, M. De Gruttola, G.P. Di Giovanni, D. Dobur, A. Drozdetskiy, R.D. Field, M. Fisher, Y. Fu, I.K. Furic, J. Gartner, J. Hugon, B. Kim, J. Konigsberg, A. Korytov, A. Kropivnitskaya, T. Kypreos, J.F. Low, K. Matchev, P. Milenovic⁵³, G. Mitselmakher, L. Muniz, R. Remington, A. Rinkevicius, P. Sellers, N. Skhirtladze, M. Snowball, J. Yelton, M. Zakaria

Florida International University, Miami, USA

V. Gaultney, L.M. Lebolo, S. Linn, P. Markowitz, G. Martinez, J.L. Rodriguez

Florida State University, Tallahassee, USA

T. Adams, A. Askew, J. Bochenek, J. Chen, B. Diamond, S.V. Gleyzer, J. Haas, S. Hagopian, V. Hagopian, M. Jenkins, K.F. Johnson, H. Prosper, V. Veeraraghavan, M. Weinberg

Florida Institute of Technology, Melbourne, USA

M.M. Baarmand, B. Dorney, M. Hohlmann, H. Kalakhety, I. Vodopyanov

University of Illinois at Chicago (UIC), Chicago, USA

M.R. Adams, I.M. Anghel, L. Apanasevich, Y. Bai, V.E. Bazterra, R.R. Betts, I. Bucinskaite, J. Callner, R. Cavanaugh, C. Dragoiu, O. Evdokimov, L. Gauthier, C.E. Gerber, S. Hamdan, D.J. Hofman, S. Khalatyan, F. Lacroix, M. Malek, C. O'Brien, C. Silkworth, D. Strom, N. Varelas

The University of Iowa, Iowa City, USA

U. Akgun, E.A. Albayrak, B. Bilki⁵⁴, W. Clarida, F. Duru, S. Griffiths, J.-P. Merlo, H. Mermerkaya⁵⁵, A. Mestvirishvili, A. Moeller, J. Nachtman, C.R. Newsom, E. Norbeck, Y. Onel, F. Ozok, S. Sen, E. Tiras, J. Wetzel, T. Yetkin, K. Yi

Johns Hopkins University, Baltimore, USA

B.A. Barnett, B. Blumenfeld, S. Bolognesi, D. Fehling, G. Giurgiu, A.V. Gritsan, Z.J. Guo, G. Hu, P. Maksimovic, S. Rappoccio, M. Swartz, A. Whitbeck

The University of Kansas, Lawrence, USA

P. Baringer, A. Bean, G. Benelli, O. Grachov, R.P. Kenny Iii, M. Murray, D. Noonan, S. Sanders, R. Stringer, G. Tinti, J.S. Wood, V. Zhukova

Kansas State University, Manhattan, USA

A.F. Barfuss, T. Bolton, I. Chakaberia, A. Ivanov, S. Khalil, M. Makouski, Y. Maravin, S. Shrestha, I. Svintradze

Lawrence Livermore National Laboratory, Livermore, USA

J. Gronberg, D. Lange, D. Wright

University of Maryland, College Park, USA

A. Baden, M. Boutemeur, B. Calvert, S.C. Eno, J.A. Gomez, N.J. Hadley, R.G. Kellogg, M. Kirn, T. Kolberg, Y. Lu, M. Marionneau, A.C. Mignerey, A. Peterman, A. Skuja, J. Temple, M.B. Tonjes, S.C. Tonwar, E. Twedt

Massachusetts Institute of Technology, Cambridge, USA

G. Bauer, J. Bendavid, W. Busza, E. Butz, I.A. Cali, M. Chan, V. Dutta, G. Gomez Ceballos, M. Goncharov, K.A. Hahn, Y. Kim, M. Klute, W. Li, P.D. Luckey, T. Ma, S. Nahn, C. Paus, D. Ralph, C. Roland, G. Roland, M. Rudolph, G.S.F. Stephans, F. Stöckli, K. Sumorok, K. Sung, D. Velicanu, E.A. Wenger, R. Wolf, B. Wyslouch, S. Xie, M. Yang, Y. Yilmaz, A.S. Yoon, M. Zanetti

University of Minnesota, Minneapolis, USA

S.I. Cooper, P. Cushman, B. Dahmes, A. De Benedetti, G. Franzoni, A. Gude, J. Haupt, S.C. Kao, K. Klapoetke, Y. Kubota, J. Mans, N. Pastika, R. Rusack, M. Sasseville, A. Singovsky, N. Tambe, J. Turkewitz

University of Mississippi, University, USA

L.M. Cremaldi, R. Kroeger, L. Perera, R. Rahmat, D.A. Sanders

University of Nebraska-Lincoln, Lincoln, USA

E. Avdeeva, K. Bloom, S. Bose, J. Butt, D.R. Claes, A. Dominguez, M. Eads, P. Jindal, J. Keller, I. Kravchenko, J. Lazo-Flores, H. Malbouisson, S. Malik, G.R. Snow

State University of New York at Buffalo, Buffalo, USA

U. Baur, A. Godshalk, I. Iashvili, S. Jain, A. Kharchilava, A. Kumar, S.P. Shipkowski, K. Smith

Northeastern University, Boston, USA

G. Alverson, E. Barberis, D. Baumgartel, M. Chasco, J. Haley, D. Nash, D. Trocino, D. Wood, J. Zhang

Northwestern University, Evanston, USA

A. Anastassov, A. Kubik, N. Mucia, N. Odell, R.A. Ofierzynski, B. Pollack, A. Pozdnyakov, M. Schmitt, S. Stoynev, M. Velasco, S. Won

University of Notre Dame, Notre Dame, USA

L. Antonelli, D. Berry, A. Brinkerhoff, M. Hildreth, C. Jessop, D.J. Karmgard, J. Kolb, K. Lannon, W. Luo, S. Lynch, N. Marinelli, D.M. Morse, T. Pearson, R. Ruchti, J. Slaunwhite, N. Valls, M. Wayne, M. Wolf

The Ohio State University, Columbus, USA

B. Bylsma, L.S. Durkin, C. Hill, R. Hughes, K. Kotov, T.Y. Ling, D. Puigh, M. Rodenburg, C. Vuosalo, G. Williams, B.L. Winer

Princeton University, Princeton, USA

N. Adam, E. Berry, P. Elmer, D. Gerbaudo, V. Halyo, P. Hebda, J. Hegeman, A. Hunt, E. Laird, D. Lopes Pegna, P. Lujan, D. Marlow, T. Medvedeva, M. Mooney, J. Olsen, P. Piroué, X. Quan, A. Raval, H. Saka, D. Stickland, C. Tully, J.S. Werner, A. Zuranski

University of Puerto Rico, Mayaguez, USA

J.G. Acosta, E. Brownson, X.T. Huang, A. Lopez, H. Mendez, S. Oliveros, J.E. Ramirez Vargas, A. Zatserklyaniy

Purdue University, West Lafayette, USA

E. Alagoz, V.E. Barnes, D. Benedetti, G. Bolla, D. Bortoletto, M. De Mattia, A. Everett, Z. Hu, M. Jones, O. Koybasi, M. Kress, A.T. Laasanen, N. Leonardo, V. Maroussov, P. Merkel,

D.H. Miller, N. Neumeister, I. Shipsey, D. Silvers, A. Svyatkovskiy, M. Vidal Marono, H.D. Yoo, J. Zablocki, Y. Zheng

Purdue University Calumet, Hammond, USA

S. Guragain, N. Parashar

Rice University, Houston, USA

A. Adair, C. Boulahouache, V. Cuplov, K.M. Ecklund, F.J.M. Geurts, B.P. Padley, R. Redjimi, J. Roberts, J. Zabel

University of Rochester, Rochester, USA

B. Betchart, A. Bodek, Y.S. Chung, R. Covarelli, P. de Barbaro, R. Demina, Y. Eshaq, A. Garcia-Bellido, P. Goldenzweig, Y. Gotra, J. Han, A. Harel, S. Korjenevski, D.C. Miner, D. Vishnevskiy, M. Zielinski

The Rockefeller University, New York, USA

A. Bhatti, R. Ciesielski, L. Demortier, K. Goulios, G. Lungu, S. Malik, C. Mesropian

Rutgers, the State University of New Jersey, Piscataway, USA

S. Arora, A. Barker, J.P. Chou, C. Contreras-Campana, E. Contreras-Campana, D. Duggan, D. Ferencek, Y. Gershtein, R. Gray, E. Halkiadakis, D. Hidas, A. Lath, S. Panwalkar, M. Park, R. Patel, V. Rekovic, A. Richards, J. Robles, K. Rose, S. Salur, S. Schnetzer, C. Seitz, S. Somalwar, R. Stone, S. Thomas

University of Tennessee, Knoxville, USA

G. Cerizza, M. Hollingsworth, S. Spanier, Z.C. Yang, A. York

Texas A&M University, College Station, USA

R. Eusebi, W. Flanagan, J. Gilmore, T. Kamon⁵⁶, V. Khotilovich, R. Montalvo, I. Osipenkov, Y. Pakhotin, A. Perloff, J. Roe, A. Safonov, T. Sakuma, S. Sengupta, I. Suarez, A. Tatarinov, D. Toback

Texas Tech University, Lubbock, USA

N. Akchurin, J. Damgov, P.R. Duderu, C. Jeong, K. Kovitanggoon, S.W. Lee, T. Libeiro, Y. Roh, I. Volobouev

Vanderbilt University, Nashville, USA

E. Appelt, D. Engh, C. Florez, S. Greene, A. Gurrola, W. Johns, C. Johnston, P. Kurt, C. Maguire, A. Melo, P. Sheldon, B. Snook, S. Tuo, J. Velkovska

University of Virginia, Charlottesville, USA

M.W. Arenton, M. Balazs, S. Boutle, B. Cox, B. Francis, J. Goodell, R. Hirosky, A. Ledovskoy, C. Lin, C. Neu, J. Wood, R. Yohay

Wayne State University, Detroit, USA

S. Gollapinni, R. Harr, P.E. Karchin, C. Kottachchi Kankanamge Don, P. Lamichhane, A. Sakharov

University of Wisconsin, Madison, USA

M. Anderson, M. Bachtis, D. Belknap, L. Borrello, D. Carlsmith, M. Cepeda, S. Dasu, L. Gray, K.S. Grogg, M. Grothe, R. Hall-Wilton, M. Herndon, A. Hervé, P. Klabbers, J. Klukas, A. Lanaro, C. Lazaridis, J. Leonard, R. Loveless, A. Mohapatra, I. Ojalvo, G.A. Pierro, I. Ross, A. Savin, W.H. Smith, J. Swanson

†: Deceased

1: Also at National Institute of Chemical Physics and Biophysics, Tallinn, Estonia

- 2: Also at Universidade Federal do ABC, Santo Andre, Brazil
- 3: Also at California Institute of Technology, Pasadena, USA
- 4: Also at CERN, European Organization for Nuclear Research, Geneva, Switzerland
- 5: Also at Laboratoire Leprince-Ringuet, Ecole Polytechnique, IN2P3-CNRS, Palaiseau, France
- 6: Also at Suez Canal University, Suez, Egypt
- 7: Also at Zewail City of Science and Technology, Zewail, Egypt
- 8: Also at Cairo University, Cairo, Egypt
- 9: Also at Fayoum University, El-Fayoum, Egypt
- 10: Also at British University, Cairo, Egypt
- 11: Now at Ain Shams University, Cairo, Egypt
- 12: Also at Soltan Institute for Nuclear Studies, Warsaw, Poland
- 13: Also at Université de Haute-Alsace, Mulhouse, France
- 14: Now at Joint Institute for Nuclear Research, Dubna, Russia
- 15: Also at Moscow State University, Moscow, Russia
- 16: Also at Brandenburg University of Technology, Cottbus, Germany
- 17: Also at Institute of Nuclear Research ATOMKI, Debrecen, Hungary
- 18: Also at Eötvös Loránd University, Budapest, Hungary
- 19: Also at Tata Institute of Fundamental Research - HECR, Mumbai, India
- 20: Also at University of Visva-Bharati, Santiniketan, India
- 21: Also at Sharif University of Technology, Tehran, Iran
- 22: Also at Isfahan University of Technology, Isfahan, Iran
- 23: Also at Shiraz University, Shiraz, Iran
- 24: Also at Plasma Physics Research Center, Science and Research Branch, Islamic Azad University, Teheran, Iran
- 25: Also at Facoltà Ingegneria Università di Roma, Roma, Italy
- 26: Also at Università della Basilicata, Potenza, Italy
- 27: Also at Università degli Studi Guglielmo Marconi, Roma, Italy
- 28: Also at Università degli studi di Siena, Siena, Italy
- 29: Also at University of Bucharest, Faculty of Physics, Bucuresti-Magurele, Romania
- 30: Also at Faculty of Physics of University of Belgrade, Belgrade, Serbia
- 31: Also at University of Florida, Gainesville, USA
- 32: Also at University of California, Los Angeles, Los Angeles, USA
- 33: Also at Scuola Normale e Sezione dell' INFN, Pisa, Italy
- 34: Also at INFN Sezione di Roma; Università di Roma "La Sapienza", Roma, Italy
- 35: Also at University of Athens, Athens, Greece
- 36: Also at Rutherford Appleton Laboratory, Didcot, United Kingdom
- 37: Also at The University of Kansas, Lawrence, USA
- 38: Also at Paul Scherrer Institut, Villigen, Switzerland
- 39: Also at Institute for Theoretical and Experimental Physics, Moscow, Russia
- 40: Also at Gaziosmanpasa University, Tokat, Turkey
- 41: Also at Adiyaman University, Adiyaman, Turkey
- 42: Also at The University of Iowa, Iowa City, USA
- 43: Also at Mersin University, Mersin, Turkey
- 44: Also at Ozyegin University, Istanbul, Turkey
- 45: Also at Kafkas University, Kars, Turkey
- 46: Also at Suleyman Demirel University, Isparta, Turkey
- 47: Also at Ege University, Izmir, Turkey
- 48: Also at School of Physics and Astronomy, University of Southampton, Southampton, United Kingdom

49: Also at INFN Sezione di Perugia; Università di Perugia, Perugia, Italy

50: Also at University of Sydney, Sydney, Australia

51: Also at Utah Valley University, Orem, USA

52: Also at Institute for Nuclear Research, Moscow, Russia

53: Also at University of Belgrade, Faculty of Physics and Vinca Institute of Nuclear Sciences, Belgrade, Serbia

54: Also at Argonne National Laboratory, Argonne, USA

55: Also at Erzincan University, Erzincan, Turkey

56: Also at Kyungpook National University, Daegu, Korea